MARTIN MARIETTA ENERGY SYSTEMS LIBRARIES
3 4456 0133957 0

CENTRAL RESEARCH LIBRARY

ORNL/NUREG/TM-25

Cy 48

Behavior of Iodine, Methyl Iodide, Cesium Oxide, and Cesium Iodide in Steam and Argon

R. A. Lorenz
M. F. Osborne
J. L. Collins
S. R. Manning
A. P. Malinauskas

OAK RIDGE NATIONAL LABORATORY
CENTRAL RESEARCH LIBRARY
DOCUMENT COLLECTION
LIBRARY LOAN COPY
DO NOT TRANSFER TO ANOTHER PERSON
If you wish someone else to see this document, send in name with document and the library will arrange a loan.
UCN-7969
(3 3-67)

OAK RIDGE NATIONAL LABORATORY
OPERATED BY UNION CARBIDE CORPORATION FOR THE ENERGY RESEARCH AND DEVELOPMENT ADMINISTRATION

Printed in the United States of America. Available from
National Technical Information Service
U.S. Department of Commerce
5285 Port Royal Road, Springfield, Virginia 22161
Price: Printed Copy $4.50; Microfiche $2.25

This report was prepared as an account of work sponsored by the United States Government. Neither the United States nor the Energy Research and Development Administration/United States Nuclear Regulatory Commission, nor any of their employees, nor any of their contractors, subcontractors, or their employees, makes any warranty, express or implied, or assumes any legal liability or responsibility for the accuracy, completeness or usefulness of any information, apparatus, product or process disclosed, or represents that its use would not infringe privately owned rights.

ORNL/NUREG/TM-25
NRC-3

Contract No. W-7405-eng-26

CHEMICAL TECHNOLOGY DIVISION

BEHAVIOR OF IODINE, METHYL IODIDE, CESIUM OXIDE, AND CESIUM IODIDE IN STEAM AND ARGON*

R. A. Lorenz
M. F. Osborne
J. L. Collins
S. R. Manning

A. P. Malinauskas, Program Manager

*This work was funded by the Nuclear Regulatory Commission under Interagency agreement 40-495-75.

Date Prepared: June 1976
Date Published: July 1976

OAK RIDGE NATIONAL LABORATORY
Oak Ridge, Tennessee 37830
operated by
UNION CARBIDE CORPORATION
for the
ENERGY RESEARCH AND DEVELOPMENT ADMINISTRATION

MARTIN MARIETTA ENERGY SYSTEMS LIBRARIES
3 4456 0133957 0

TABLE OF CONTENTS

PAGE

ABSTRACT 1

1. INTRODUCTION 2

2. EXPERIMENTS WITH ELEMENTAL IODINE 5

2.1 Introduction 5
2.2 Behavior of I_2 in Argon at 800°C (Control Test 1). . . . 7
2.3 Behavior of I_2 in Steam at 800°C (Control Test 2). . . . 7
2.4 Behavior of I_2 in Steam at 800°C (Control Test 3). . . . 11
2.5 Conclusions 13

3. EXPERIMENTS WITH METHYL IODIDE 13

3.1 Introduction 13
3.2 Behavior of CH_3I in Steam at 800°C (Control Test 4). . . 14
3.3 Behavior of CH_3I in Steam at 500°C (Control Test 5). . . 15
3.4 Behavior of CH_3I in Steam at 600°C (Control Test 6). . . 17
3.5 Conclusions 17

4. EXPERIMENTS WITH CESIUM MONOXIDE 19

4.1 Introduction 19
4.2 Behavior of Cs_2O in Steam at 700°C (Control Tests 7 and 8) 19
4.3 Behavior of Cs_2O in Steam at 700, 800, and 950°C (Control Test 9) 23
4.4 Conclusions 26

5. EXPERIMENT WITH CESIUM IODIDE 26

5.1 Introduction 26
5.2 Behavior of CsI in Steam at 700°C (Control Test 10). . . 26

6. PERFORMANCE OF THE APPARATUS 32

6.1 General Analysis 32
6.2 Quartz Furnace Tube and Quartz Liner 32
6.3 Thermal Gradient Tube 33
6.4 Low-Pressure Cascade Impactor 34
6.5 High-Efficiency Filters 35
6.6 Silver-Plated Screens 36
6.7 Adsorbers. 38

PAGE

7. APPLICATION OF RESULTS 40

7.1 Application to Future Experiments with H. B. Robinson Irradiated Fuel 40
7.2 Application of Results to Reactor Safety Analysis . . 42

8. REFERENCES 43

BEHAVIOR OF IODINE, METHYL IODIDE, CESIUM OXIDE, AND CESIUM IODIDE IN STEAM AND ARGON

R. A. Lorenz
M. F. Osborne
J. L. Collins
S. R. Manning

A. P. Malinauskas, Program Manager

ABSTRACT

An experimental program has been initiated with the overall goal of providing a definitive understanding of fission product behavior under conditions applicable to light water reactor accidents in which the fuel rods reach a maximum temperature in the range 500 to 1300°C. In order to test the apparatus and techniques of analysis, a series of ten experiments was performed in which selected fission product-type compounds were exposed to high-temperature steam and argon atmospheres.

The species investigated were I_2, CH_3I, Cs_2O, and CsI, mainly in a steam atmosphere over the temperature range 500 to 950°C. The collection apparatus consisted of a thermal gradient tube for deposition of compounds condensable above 125°C, a low-pressure cascade impactor and high-efficiency filters for collection of particulate material, silver-plated screens for the collection of reactive forms of iodine, impregnated charcoal and silver-exchanged zeolite for trapping organic iodides, and cold charcoal (which can be used for the collection of noble gases).

The apparatus performed satisfactorily, but some revisions were made to reduce the extraneous adsorption of I_2 on metal and filter fiber surfaces. Further reductions in both size and surface area were projected as necessary for reliable analysis of ^{129}I from irradiated fuel samples in cases where the mass of collected ^{129}I would be less than the order of 10 μg.

Iodine remained stable at 800°C in steam and argon, but CH_3I decomposed; decomposition rate constants were calculated. Cesium monoxide reacted rapidly with steam to form CsOH (probably the monohydrate) which, in turn, reacted with the quartz furnace tube. Cesium iodide in steam at 700°C decomposed partially by reaction with quartz. Although most of the CsI and the unreacted CsOH was collected in the thermal gradient tube, a small fraction of both these compounds was deposited in the form of particles in the cascade impactor and on the filters.

1. INTRODUCTION

The main objectives of the program are to determine, with greater precision, the quantities of radiologically significant fission products that can be released under successfully terminated loss of coolant accident (LOCA) and postulated spent fuel transportation accident (SFTA) conditions, and to identify these species with respect to both chemical and physical forms. Toward these ends, an apparatus has been designed and constructed and is currently being utilized in a research program which consists of a progression of experiments that will ultimately involve the use of high-burnup, light water reactor (LWR) fuel rod segments. Emphasis is given to the steam environment and temperatures below 1500°C.

The Control Test Series, the first series of experiments in this progression, was conducted to determine the effect of high-temperature steam environments (500 to 950°C in the furnace tube) on known fission product compounds, to evaluate the effectiveness of the apparatus arrangement, and to gain experience in the utilization of different analytical methods in the identification of the released species.

This series included testing with I_2, CH_3I, Cs_2O, and CsI. The modes of introducing these materials into the hot furnace tube are discussed in detail in Sects. 2-5. The most efficient arrangement of apparatus developed as the result of the Control Test Series is shown in Figs. 1 and 2. The components shown in Fig. 2 are as follows: (1) furnace tube heater, (2) quartz furnace tube, (3) gas inlet of furnace tube, (4) quartz liner for furnace tube, (5) fuel rod assembly (not used in Control Test Series), (6) connector for pressurizing fuel rod, (7) Chromel-Alumel thermocouples, (8) induction coil heater (not used in Control Test Series), (9) thermal gradient heater assembly, (10) gold thermal gradient tube in quartz tube housing, (11) orifice assembly (includes orifice plate), (12) orifice plate, (13) impactor housing, (14) impactor stages (membrane collector included), (15) filter housing, (16) filter papers (2), (17) silver screens (12), (18) adsorber housing, (19) adsorbers: 3 charcoal cartridges and 1 silver zeolite cartridge, (20) condenser housing, and (21) Pyrex graduate for collecting condensate.

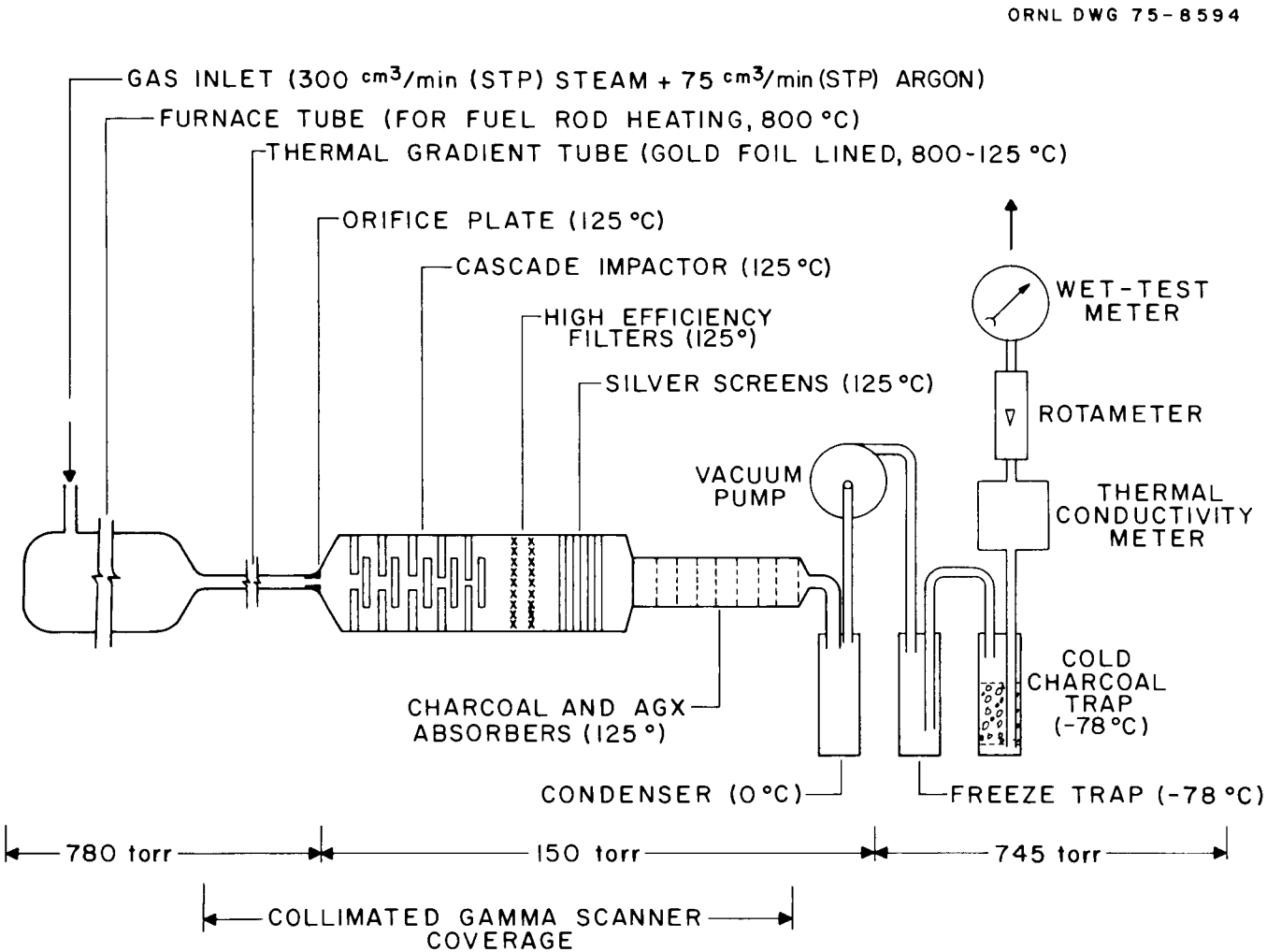

Fig. 1. Flow diagram of the collection system.

ORNL PHOTO: 0834-76A

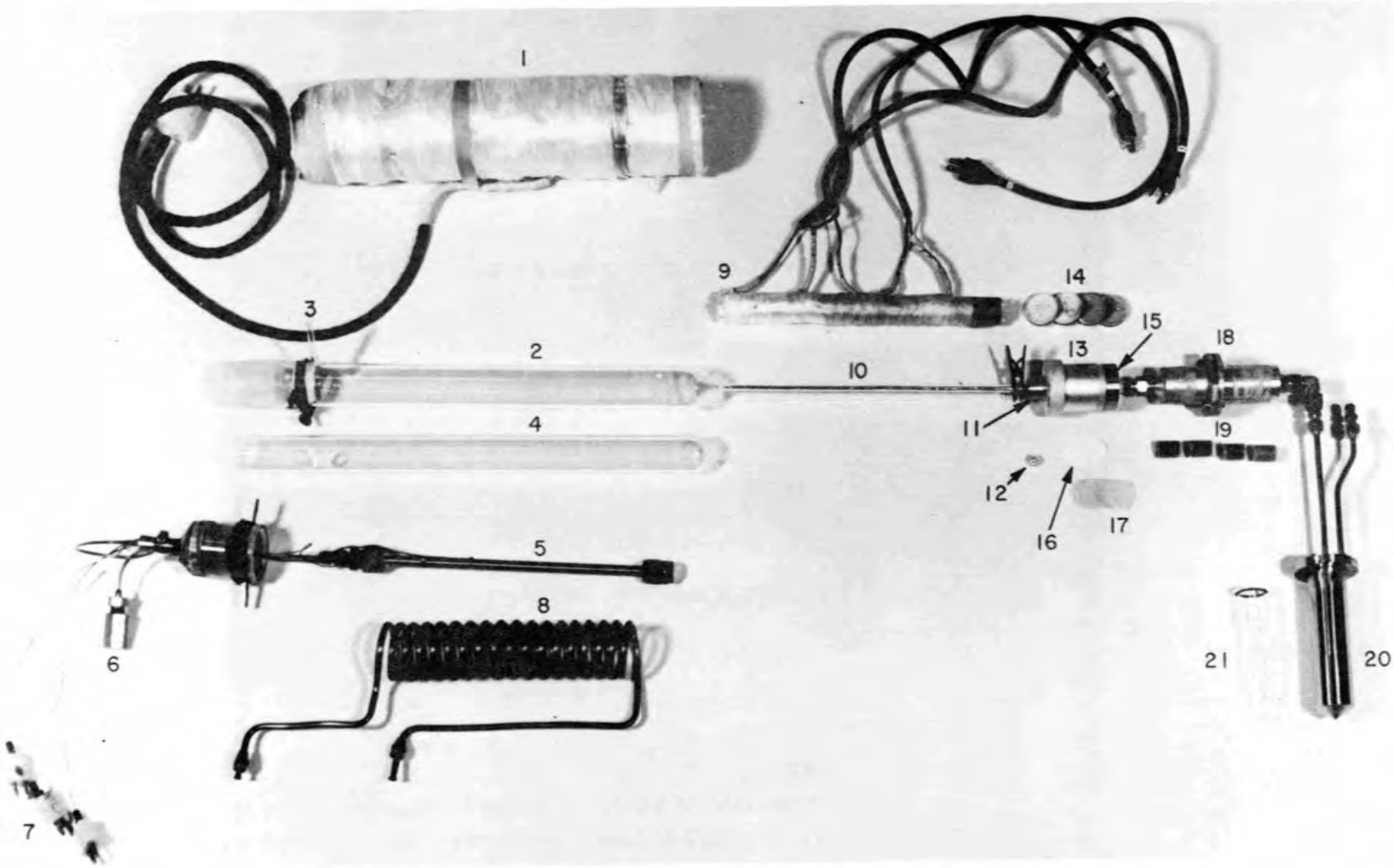

Fig. 2. Experimental apparatus used in Control Tests 1-10.

The first component of the collection-characterization system is a gold foil-lined thermal gradient tube; species with dew points above 125°C deposit by condensation in this region. A low-pressure cascade impactor located downstream from the thermal gradient tube separates particulates into five particle size fractions on Teflon membranes, which can be removed to allow direct examination of the deposited material. The low pressure permits the collection of smaller particles. Beyond the cascade impactor is a filter-pack which completes the collection of particulates on high-efficiency filter papers (2 or 3) and fine-mesh silver-plated screens (normally 12) which collect reactive iodine forms (such as I_2 and HI). Three charcoal cartridges and one silver-exchanged zeolite adsorber cartridge collect the less reactive, more penetrating chemical forms of iodine such as CH_3I. The apparatus is equipped with cold traps which may be used to collect noble gases, a thermal conductivity meter for monitoring hydrogen produced from the steam-Zircaloy reaction in later tests, and a wet-test meter for measuring larger amounts of hydrogen. A summary of the operating conditions for each of the experiments is given in Table 1.

2. EXPERIMENTS WITH ELEMENTAL IODINE

2.1 Introduction

The elemental form of iodine is commonly encountered in fission product experimentation. It is a grayish-black, lustrous solid that melts at 113.6°C and boils at 184.4°C. The vapor pressure of the solid is given[1] by the equation

$$\log P_{atm} = -3512.8/T + 2.013 \log T + 13.3740.$$

Slight hydrolysis occurs when I_2 is dissolved in water (0.029 g per 100 g of H_2O at 20°C) in accordance with the equation

$$I_2 + H_2O \rightarrow HIO + H^+ + I^-.$$

The hydrolysis constant for the reaction is calculated to be 4.6×10^{-13} at 25°C.[2]

Elemental iodine traced with ^{131}I, which was used in the control experiments, was prepared by decomposing PdI_2 at 350°C under vacuum and collecting the iodine vapor in liquid nitrogen-cooled Pyrex ampules with

Table 1. Summary of experimental operating conditions

	Experiment number									
	1	2	3	4	5	6	7	8	9	10
Control species	I_2	I_2	I_2	CH_3I	CH_3I	CH_3I	Cs_2O	Cs_2O	Cs_2O	CsI
Mass Cs, mg	0	0	0	0	0	0	13.9	14.0	5.0	0.67
Mass I, mg	0.7	3.2	3.0	4.0	3.4	5.1	0	0	0	0.64
Temperature-time, °C-hr	800-1	800-1	800-1	800-1	500-1	600-1	700-1	700-1	700-1 800-1 950-1	700-1
Steam flow rate, cm^3/min (STP)	0	528	528	278	268	299	226	305	294	277[a]
Argon flow rate, cm^3/min (STP)	330	132	132	93	89	49	57	62	64	52[a]
Furnace tube pressure, torr	755	755	820	760	770	760	760	755	760	750
Impactor pressure, torr	161	161	161	161	161	161	161	161	186	186
Adsorber assembly pressure, torr	745	745	161	161	161	161	161	161	186	186
Amount of original source material found at end of experiment, %[b]	-	72	97	82	101	102	99	104	84	67

[a]Steam and argon inflow rates; only 41% of the expected condensate volume was collected, indicating a leak in the system, probably at the furnace tube cap.

[b]Leakage at the furnace tube end cap probably accounts for the occasional loss of material shown. Tables 2, 3, and 5 are based on the amount of material found at the end of the experiment. No loss of material during disassembly and counting was detected.

breakable seals after removal of volatile contaminants such as CH_3I. A detailed procedure of the preparation of elemental iodine by PdI_2 decomposition is described by Osborne et al.[3] In each experiment, the ampule was placed in a Pyrex tube assembly attached to the gas inlet line of the furnace tube (Fig. 2). A magnet was used to move a small, plastic-coated iron rod in the assembly to break the ampule seal. In each experiment, the iodine source was gently heated so that the I_2 was injected into the furnace tube essentially on a continuous basis for the first 15 min. Summaries of the operating conditions and results are given in Tables 1 and 2, respectively.

2.2 Behavior of I_2 in Argon at 800°C (Control Test 1)

This experiment was concerned with the behavior of elemental iodine (I_2) in an atmosphere of pure, dry argon. The distribution of iodine in the apparatus was typical for elemental iodine, except for a deposit which peaked at 330°C in the gold thermal gradient tube (see Fig. 3). The deposited material could not be identified by x-ray fluorescence analysis, apparently because of low concentration. No particulate iodine was found in the cascade impactor or on the high-efficiency filter papers. A large amount of iodine collected in these assemblies as the result of sorption of I_2 on the various metal and filter fiber surfaces, which is typical behavior for I_2.[4,5] As shown in Fig. 4, distribution data for the series of charcoal adsorber cartridges indicated the presence of a small fraction of iodine more penetrating than elemental iodine. Most of the elemental iodine was collected in the first charcoal cartridge.

2.3 Behavior of I_2 in Steam at 800°C (Control Test 2)

In this test, elemental iodine was injected into a flowing 80% steam--20% argon mixture. The deposition of iodine in the collection system was again as expected for elemental iodine. A deposition which occurred in the thermal gradient tube at approximately 200°C was broader than the one that developed in the first control test, presumably because of higher velocity. A stainless steel adapter added to the orifice assembly with the objective of minimizing stresses in the quartz thermal

Table 2. Distribution of iodine in c[illegible] $_2$ or CH_3I

Location	Temperature (°C)	Percent in each location: 800°C Furnace Control 1 (I_2)	800°C Furnace Control 2 (I_2)	800°C Furnace Control 3 (I_2)	800°C Furnace Control 4 (CH_3I)	500°C Furnace Control 5 (CH_3I)	600°C Furnace Control 6 (CH_3I)
Furnace tube	500-800	18.3	4.1	31.4	5.3	1.5	4.6
Thermal gradient tube	125-800	3.7	2.0	2.3	0.74	0.96	a
Orifice assembly	125	0.94	42.5	10.0	11.4	0.48	3.2
Impactor housing	125	16.4	26.3	17.5	5.5	2.4	0.78
First-stage paper		0.04	0.09	0.039	0.03	0.03	a
Second-stage paper		0.02	0.21[b]	0.021	9.9[c]	0.02	a
Third-stage paper		0.05	0.017	0.021[c]	0.02	0.007	a
Fourth-stage paper		0.02	0.009	0.010	3.0[c]	0.003	a
Fifth-stage paper		0.12	0.009	0.023	0.03	0.0005	a
Filter housing	125	25.2	4.2	8.2	3.2	1.9	3.1
First filter paper[d]		14.8	1.9	1.3	0.21	0.04	0.11
Second filter paper[d]		7.0	1.7	0.54	0.16	0.02	0.09
Silver screens No. 1		-	-	15.5	13.0	4.3	11.0
No. 2		-	-	9.3	12.1	1.4	10.9
Nos. 3-5		-	-	3.3	33.5[e]	0.1[f]	48.4[f]
Condenser housing (Tests 1 and 2)	0	9.2	7.9	-	-	-	-
Condensate		-	0.34	-	-	-	-
Adsorber housing	g	2.6	1.6	0.01	0.005	1.5	0.56
Charcoal[h] No. 1		1.5[i]	7.1[i]	0.005	2.0	85.3	11.2
No. 2		0.06[i]	0.01[i]	0.071	0.003	0.01	5.8
No. 3		0.006[i]	0.013[i]	0.003	0.001	0.001	0.03
No. 4		0.001[i]	0.0002[i]	0.003	0.0005	0.001	0.03
Other adsorbers		0.003	0.011	0.013	0.002	0.005	0.08
Condenser housing (Tests 3-6)	0	-	-	< 0.32	< 0.002	< 0.004	< 0.003
Condensate		-	-	< 0.41	< 0.002	< 0.004	< 0.003
Freeze trap	-78	< 0.001	< 0.0004	< 0.003	< 0.002	< 0.002	< 0.0003
Cold charcoal trap	-78	< 0.0004	< 0.0001	< 0.006	< 0.004	< 0.004	< 0.0006

[a]Gold liner and impactor stages omitted since the objective of the experiment was to measure CH_3I decomposition.
[b]Nuclepore filter paper.
[c]Nylon filter paper.
[d]Cambridge type 1G.
[e]Nos. 3-7 silver screens.
[f]Nos. 3-12 silver screens.
[g]25°C in tests 1 and 2; 125°C in tests 3-6.
[h]G-618, impregnated with 5% triethylenediamine (TEDA).
[i]WITCO Grade 42, 12-16 mesh.

ORNL-DWG 76-816

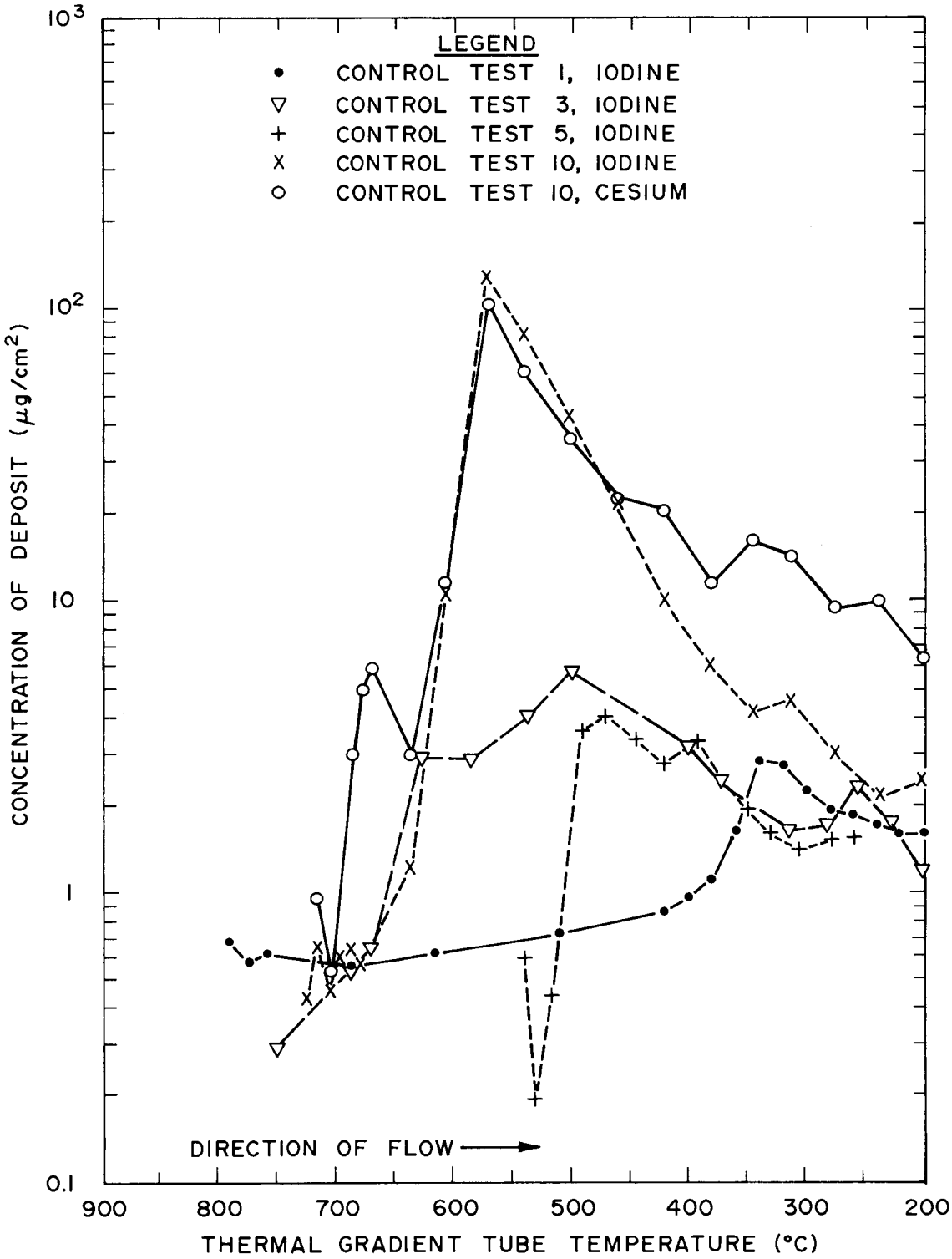

Fig. 3. Deposition of iodine-containing compounds in the thermal gradient tube.

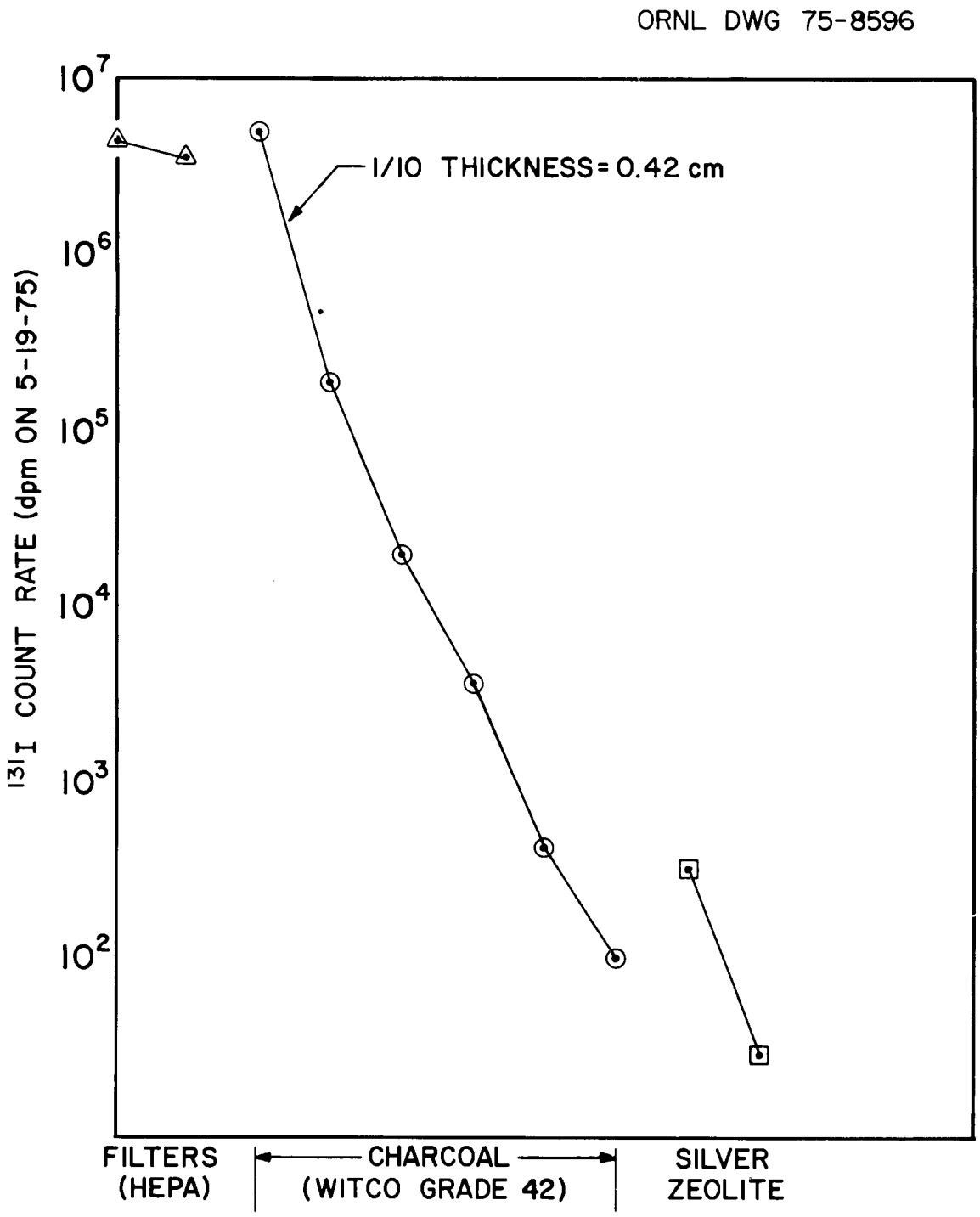

Fig. 4. Iodine distribution in the adsorber pack from Control Test 1.

gradient tube proved to be a primary point of iodine absorption. Approximately 42.5% of the iodine deposited on the orifice assembly, which included the adapter (see Table 2).

The lack of a thermocouple at this position makes it impossible for us to know whether the temperature was low enough to permit steam condensation, which would provide a more conducive condition for iodine deposition. The particle filter assembly was redesigned for this test; the smaller filter papers and fewer supporting screens that were employed succeeded in reducing the total sorption of iodine by this assembly. As was the case in Control Test 1, the impactor and filters revealed no evidence of particulate iodine. Excessive scatter occurred in the charcoal adsorber data, possibly because of entrained condensate.

2.4 Behavior of I_2 in Steam at 800°C (Control Test 3)

To eliminate the ambiguity of the chemical forms of iodine collected in the condenser and charcoal adsorbers, as seen in the first two experiments, five silver-plated 80 mesh screens were placed in the filter assembly following the high-efficiency filter papers. Silver screens with cleaned surfaces have a reputation of being very efficient at removing reactive iodine forms such as I_2 and HI; thus the use of silver-plated screens should allow only penetrating forms such as CH_3I to reach the charcoal adsorber cartridges.[4] The adsorbers were moved upstream of the condenser and were heated so that only very highly penetrating forms of iodine could reach the condenser. The stainless steel adapter used in Control Test 2 was omitted, and the orifice assembly was modified to reduce the sorption of I_2.

The operating conditions in this experiment were the same as those of Control Test 2 (see Table 1); the results are presented in Table 2. As in Control Tests 1 and 2, no particulate iodine (only sorbed iodine) was found in the impactor or on the high-efficiency filter papers. The first two silver screens were nearly saturated with iodine, with coverage of the order of 70 monolayers* (Fig. 5). Iodine was found unexpectedly in the condensate (pH 9.0); however, since it is possible that an undetected residue remained from previous tests, we have listed a maximal value in Table 2.

*A monolayer coverage of iodine is about 0.3 $\mu g/cm^2$.[6]

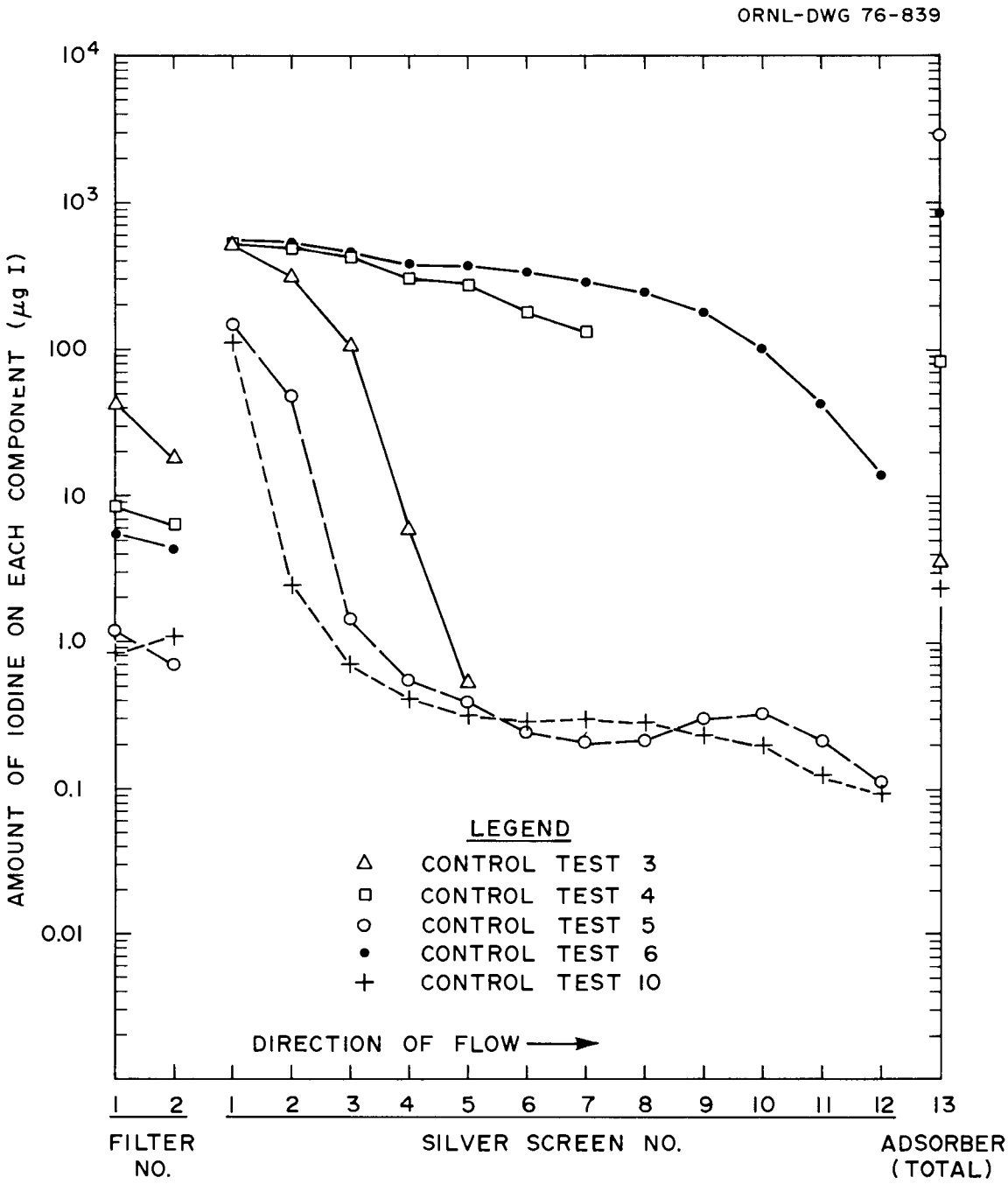

Fig. 5. Iodine retained on particulate filters and silver-plated screens.

In this and succeeding experiments, we began using a type of charcoal suitable for direct neutron activation. This technique will allow us to analyze for the ^{129}I that is expected to be collected during subsequent experiments with irradiated fuel. A batch of type G-618 charcoal (North American Carbon Company) was tested and found to contain low concentrations of elements that would interfere with ^{130}I (12.4-hr half-life) counting. This charcoal is impregnated with 5% triethylenediamine (TEDA) to chemically trap CH_3I. The batch was screened to obtain a small particle size (12-16 mesh) for high adsorption efficiency.

Charcoals which contain TEDA concentrations of the order of 5% are excellent collectors of CH_3I but suffer the disadvantage of loss of impregnant at perhaps 150°C or higher and ignition (in air) at temperatures occasionally as low as 190°C.[7,8]

2.5 Conclusions

The elemental iodine behaved more or less as expected in each of the three control tests. It adsorbed on the metal surfaces (aluminum, silver, and stainless steel), filter fibers, and adsorbers (impregnated charcoal and silver-exchanged zeolite) in typical fashion. The equipment modifications and rearrangement made for Control Test 3 proved to be very effective and were therefore used for succeeding experiments. The more compact arrangement of equipment should be especially advantageous in instances where experiments are performed with low- and high-burnup fuel rod segments since these contain ^{129}I, which can only be measured at low concentrations by neutron activation analysis.

3. EXPERIMENTS WITH METHYL IODIDE

3.1 Introduction

In a recent review[9] of organic iodide formation under postulated accident conditions in water-cooled reactors, Postma and Zavadoski concluded that less than 1% of the iodine initially airborne (initial concentration, 100 mg/m^3) could be converted to organic iodides by nonradiolytic means, and that, during the first 2 hr following fission product release, gas-phase radiolytic formation would add no more than 2.2% to the conversion. Gevatman and Williams pointed out that the

decomposition products of organic materials (lubricants) and trace-level contaminants in the earth's atmosphere are the potential organic sources within a containment vessel available to react with elemental iodine to produce organic iodides, the predominant one being CH_3I.[10]

Methyl iodide boils at 42.5°C and freezes at -66°C. Its vapor pressure[11] is given by the equation

$$\log_{10} P_{mm} = -\frac{1475}{T} + 7.56.$$

Between 4.8 and 29.9°C, the partition coefficient at equilibrium[12] (β) can be calculated from the equation

$$\log (\beta) = -4.82 + \frac{1597}{T},$$

where T is the temperature in K. An excellent discussion of the chemical and physicochemical properties of methyl iodide is given in a Nuclear Safety Information Center (NSIC) report[13] by Parsly.

In Control Tests 4-6, our primary objective was to determine the behavior of CH_3I in high-temperature steam. We were also interested in the efficiency of the charcoal and silver zeolite adsorbers which operate at low pressure in our apparatus. In each of the experiments, the desired quantity of CH_3I was slowly released from a gas cylinder into the inlet line of the furnace tube. This allowed it to mix with the steam-argon stream before reaching the hot zone of the furnace tube. Summaries of the operating conditions and results are given in Tables 1 and 2, respectively.

3.2 Behavior of CH_3I in Steam at 800°C (Control Test 4)

Examination of the results in Table 2 reveals that CH_3I readily decomposed in an 80% steam--20% argon atmosphere at 800°C. Most of the iodine that deposited (∿ 80%) in the collection train was found on the metal housing surfaces and the silver screens. The deposition pattern is typical of that for chemically reactive elemental iodine (see results for Control Test 3 in Table 2) and HI.

With our present apparatus arrangement, only nonreactive chemical forms such as the surviving CH_3I should reach the adsorbers; in this test, however, some reactive iodine found its way to the adsorbers

because an insufficient number of silver-plated screens was used (see Fig. 5).

In this experiment a portion of the decomposition product behaved differently; that is, mild reaction with the stainless steel orifice housing occurred, as evidenced by the presence of a reddish-brown deposit and by an almost quantitative reaction with the first of two nylon membrane filter papers being tested as particle collection surfaces in the cascade impactor. Teflon filter papers were used in the other three stages of the cascade impactor. The first nylon paper, which was in stage 2, turned yellow and appeared to be thinned; the second paper, which was in stage 4, showed some yellowing but no thinning (Fig. 6). This behavior had not been observed in any of the previous elemental iodine tests (Control Test 3 contained one nylon paper) but was duplicated later in the laboratory. A small drop of HI was placed in contact with a piece of nylon filter paper; the resultant yellowing and thinning were similar to that noted for the first nylon paper. As reported in the literature and confirmed in the laboratory, HI reacts with stainless steel. Therefore, we believe that the decomposition product contained some HI.

3.3 Behavior of CH_3I in Steam at 500°C (Control Test 5)

Control Test 5 was made to further investigate the decomposition behavior of CH_3I in steam at a lower temperature. Table 2 shows that, although some decomposition occurred, 85.3% of the CH_3I penetrated the system before becoming adsorbed by the first charcoal cartridge. The distribution pattern of the iodine collected on the silver screens was similar to that for I_2 in Control Test 3 (Fig. 5).

In this experiment, Teflon filter papers (instead of nylon filter papers) were used in all five stages of the impactor as collection surfaces. In order to prevent possible unrecognized reactions with binder material in the Cambridge filter papers, we switched to 100% pure borosilicate glass fiber filters for this and subsequent experiments. There was no evidence of collected particulate material. No visible signs of the HI reaction with stainless steel surfaces that occurred in Control Test 4 were observed.

ORNL PHOTO 3634-75

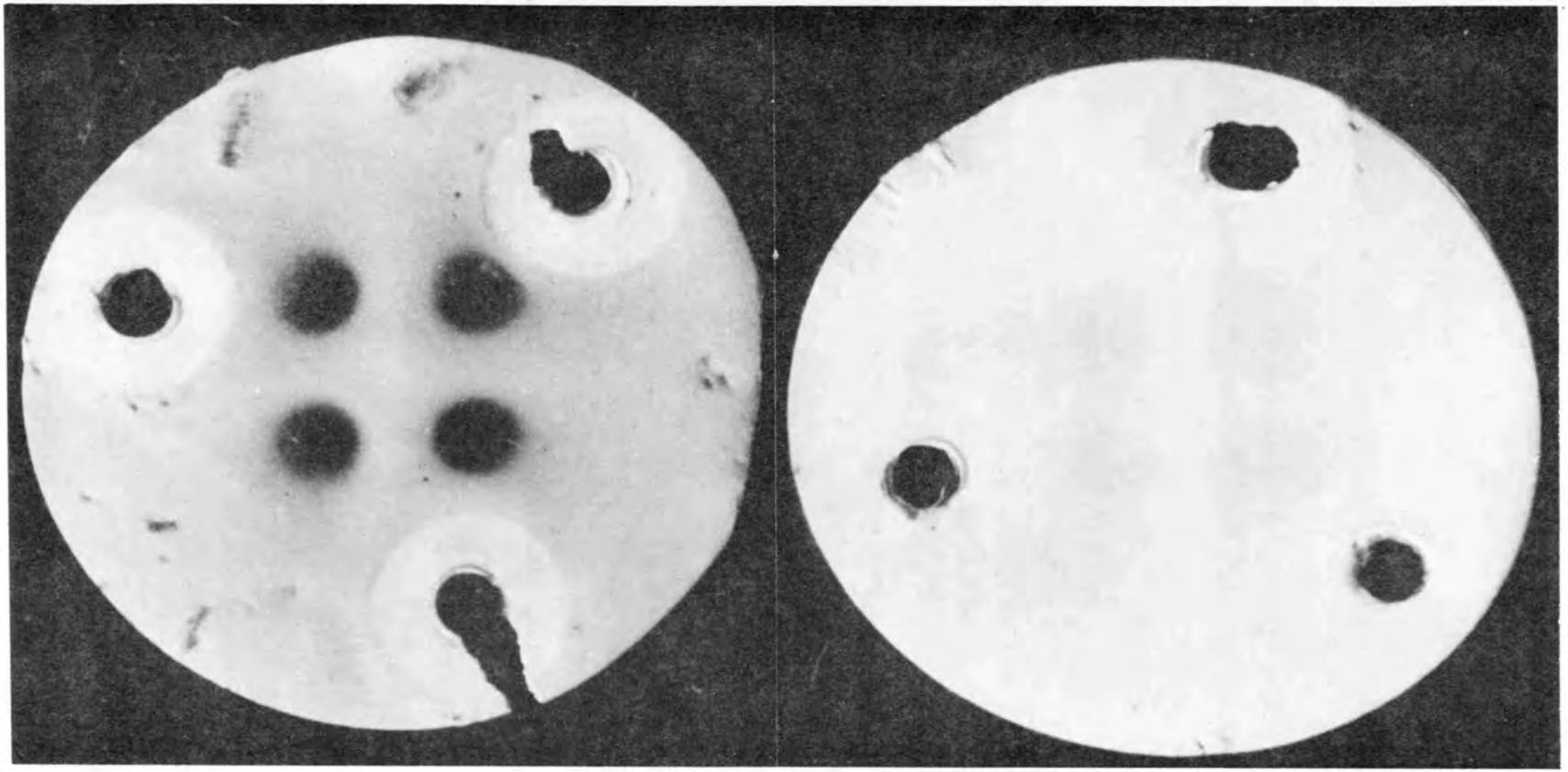

Fig. 6. Reaction of nylon membrane filter media with decomposed methyl iodide (probably HI).

3.4 Behavior of CH_3I in Steam at 600°C (Control Test 6)

This experiment was conducted to provide information about the decomposition of CH_3I in steam at an intermediate temperature between 800°C (Control Test 4), a temperature of essentially complete dissociation, and 500°C (Control Test 5), a temperature of low dissociation. Summaries of the operating conditions and results are given in Tables 1 and 2, respectively. Extensive dissociation of CH_3I is indicated in Table 2 and Fig. 5 by the large iodine deposits on the silver screens and metal housings. Only 17% of this species escaped dissociation and penetrated the collection system to the charcoal cartridges. Overheating of the adsorber assembly prior to the start of the experiment is the most credible explanation for the deeper penetration of the CH_3I into the charcoal adsorbents. Volatilization of some of the organic activating agent in the charcoal rendered the charcoal a less efficient adsorbent. In Control Test 5, all the CH_3I deposited in the first charcoal cartridge.

The gold liner of the thermal gradient tube and the impactor stages were omitted in this experiment since our objective here was simply to measure CH_3I decomposition. Again, no visible signs of the HI reaction with stainless steel surfaces that occurred in Control Test 4 were noted.

3.5 Conclusions

The decomposition of CH_3I becomes significantly greater at higher temperatures, as indicated by the iodine fraction that collected on the charcoal adsorbers: 87% at 500°C, 17% at 600°C, and 2.1% at 800°C. Only nonreactive chemical forms such as the surviving CH_3I should reach the adsorbers as the result of our modified apparatus arrangement.

By using the fraction of CH_3I that decomposed and the residence time in the high-temperature furnace, we calculated first-order decomposition rates and compared them with literature rates for decomposition in dry atmospheres,[14-16] as seen in Fig. 7. Since they are essentially identical, we conclude that steam does not accelerate the decomposition of CH_3I but does participate as a scavenger for the radicals from the cracked CH_3I molecules. Figure 7 shows that, based on literature rates,[17] hydrolysis in liquid water is a much faster reaction.

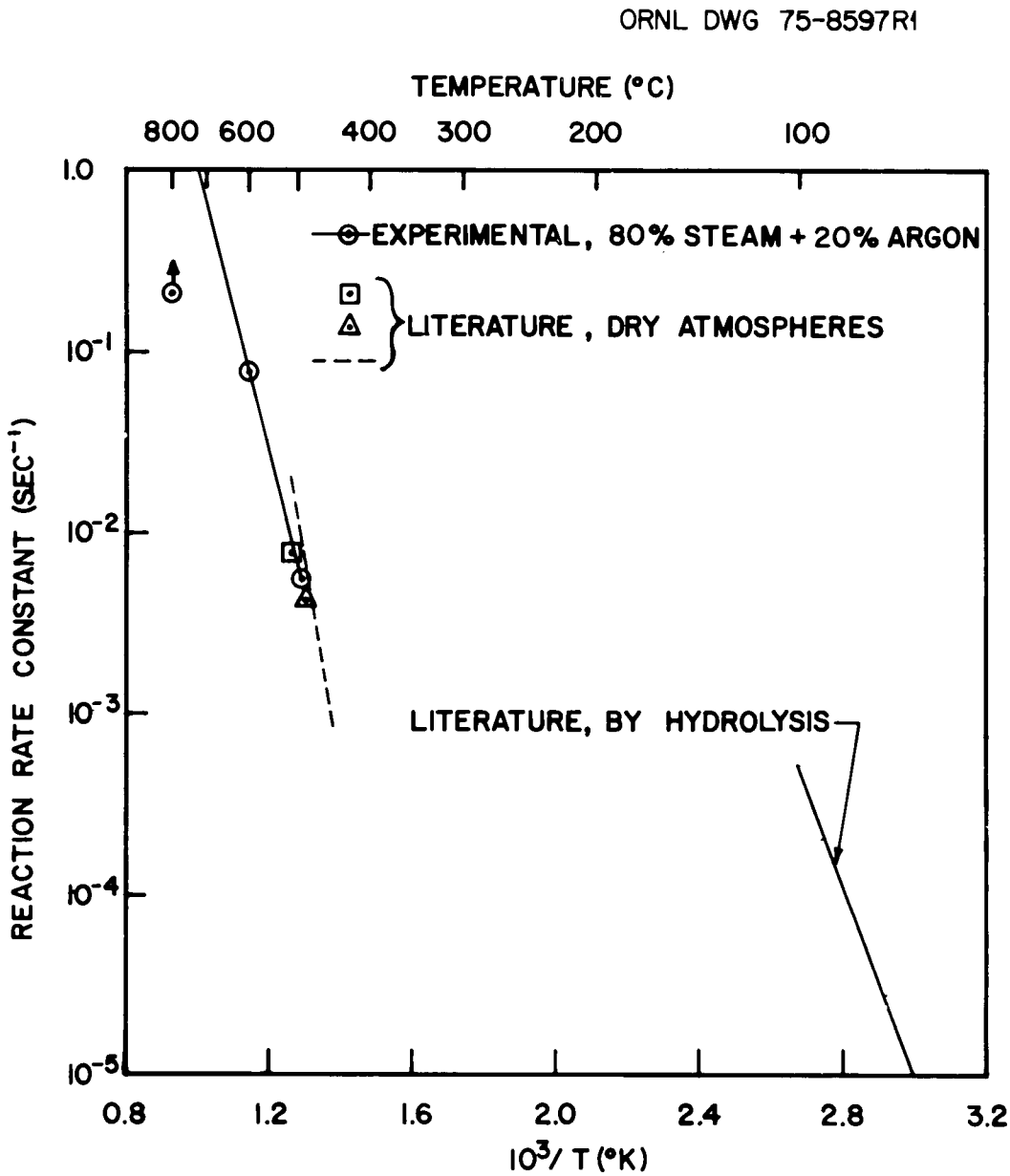

Fig. 7. Rate of decomposition of methyl iodide.

4. EXPERIMENTS WITH CESIUM MONOXIDE

4.1 Introduction

Cesium monoxide (Cs_2O) vaporizes markedly at 250°C[18] and tends to decompose into cesium metal and cesium peroxide (Cs_2O_2) at temperatures greater than 400°C. When exposed to dry air, it rapidly forms a mixture of Cs_2O_2 and cesium superoxide (CsO_2). Cs_2O combines rapidly with water to form $CsOH \cdot H_2O$ (hydrated oxide) which melts at 180°C and loses H_2O only at 400°C or higher.

Anhydrous cesium hydroxide (CsOH) is hygroscopic and the strongest base of the alkali metal group. A thermally stable compound, it retains hydrogen without loss of water well past its melting point (272°C) and volatilizes as the hydroxide, rather than first dehydrating and then volatilizing as the oxide.[19] It reacts with certain oxides of interest such as the oxides of aluminum, tin, zirconium, molybdenum, silicon (quartz), and uranium to form cesium aluminate,[19] stannate,[19] zirconate,[19,20] molybdate, silicate[21] (many forms), and uranate[22] (many forms), respectively.

Control Tests 7, 8, and 9 were performed to study the behavior of Cs_2O in an 80% steam--20% argon atmosphere at temperatures that might develop in a successfully terminated LOCA. Cesium monoxide is one of the chemical forms of cesium that could be present in a spent fuel rod. Specimens for these control tests were prepared by pyrolyzing cesium oxalate (traced with ^{137}Cs) under vacuum at 625°C and sealing in quartz ampules. Because of extensive reaction between Cs_2O (or possibly cesium carbonate, the intermediate chemical form) and the quartz ampules, most of the specimens were unusable; however, a few ampules showed the effect of only minimal reaction (etching of inner surface), and these were used in the Control Tests. Summaries of the experimental conditions and results are given in Tables 1 and 3, respectively.

4.2 Behavior of Cs_2O in Steam at 700°C (Control Tests 7 and 8)

In Control Tests 7 and 8, difficulty was encountered in breaking the Cs_2O-containing ampules enclosed within a Teflon tube attached to the gas inlet of the furnace tube (see Fig. 1) and getting the broken sections to fall down a quartz chute into the hottest area of

Table 3. Distribution of cesium in control tests using Cs_2O

Location	Temperature (°C)	Percent found in each location		
		Test 7	Test 8	Test 9
Source ampule pieces	125, 700	56.424	6.557	-
Teflon tube	125	0.543	1.820	-
Platinum boat	700	-	-	1.081
Furnace tube	700	42.815	90.924	46.813
Thermal gradient	700-165	0.027	0.408	42.467
Orifice assembly	125	0.005	0.086	0.356
Impactor housing	125	0.037	0.15	0.735
First-stage paper		0.0014	0.003[a]	0.595[b]
Second-stage paper		0.0012	0.025	0.508[b]
Third-stage paper		0.0007	0.004	0.515[b]
Fourth-stage paper		0.0004	0.002[a]	0.812[b]
Fifth-stage paper		0.0003	0.002[a]	1.604[b]
Filter housing	125	c	0.00009	0.227
First filter paper[b]		0.0005	0.0084	4.078
Second filter paper[b]		0.00002	0.0001	0.009
Silver screens, No. 1	125	0.00001	0.000	0.0132
No. 2		d	0.000	0.0066
Nos. 3-12		0.00027	0.000	0.1167
Adsorber housing	c	c	0.000	c
Charcoals No. 1		0.00009	0.000	0.0004
No. 2		0.00002	0.000	0.0003
No. 3		0.000	0.000	0.000
No. 4		0.000	0.000	0.000
Other adsorbers		0.00009	0.000	0.000
Condenser housing	0	c	≤0.007	≤0.062
Condensate		0.054	0.0001	0.0008
Freeze trap	-78	0.00009	0.000	0.000
Cold charcoal trap	-78	0.000	0.000	0.000

[a]Nuclepore membrane filter paper.
[b]Reeve Angel 934 AH, 100% borosilicate glass fiber filter paper.
[c]Not counted.
[d]Silver screen No. 2 is included with Nos. 3-12.

the furnace tube. Most of the ^{137}Cs activity after Control Test 7 was located on the pieces of broken ampule. Very little of the material that escaped from the ampules was transported beyond the furnace tube (see Table 3); most of the released cesium reacted with the gas inlet portion of the furnace tube and the quartz liner (see Fig. 2). Much of this reaction took place in the region that was at a temperature of approximately 125°C, and not in the hot zone (700°C) of the furnace tube. In Control Test 8, the ampule was broken into several small pieces, providing a more rapid release of the oxide into the steam-argon flow. At the completion of the experiment most of the cesium was found at the extensively etched gas inlet of the furnace tube, a location intermediate in temperature between the 125°C and the 700°C furnace tube.

Our explanation for this behavior is that the Cs_2O, on exposure to steam, readily formed CsOH ($CsOH \cdot H_2O$ below 400°C), which reacted with the quartz surfaces to form refractory cesium silicate.[21] Deposits taken from the furnace tube and a piece of the broken ampule at the conclusion of Control Test 7 yielded distinctive x-ray diffraction patterns of considerable complexity that could not be identified. However, we believe that these deposits are primarily mixtures of silicate.[21] The type of cesium silicate formed (many different cesium silicates are possible) would depend on the conditions of the reaction (temperature, concentration of reactants, moisture, etc.). Owing to the lack of reference standards for x-ray diffraction patterns of deposits taken from various apparatus components, we prepared compounds of likely chemical forms to use as reference materials. On this basis, we were able to identify a hydrated cesium hydroxide, probably the monohydrate, that we will designate as $CsOH \cdot xH_2O$. In Control Test 8, the hydrates were identified in deposits in the gas inlet of the furnace tube and on the second impactor stage collection paper. Scanning electron microscope (SEM) analysis revealed the presence of silicon and cesium on stage 2.

Figure 8 shows the distribution of a cesium-containing aerosol among the stages of the cascade impactor for Control Tests 7 and 8. The mass median diameters are approximately 0.35 and 0.4 μ, respectively, assuming a particle density of 3.6.

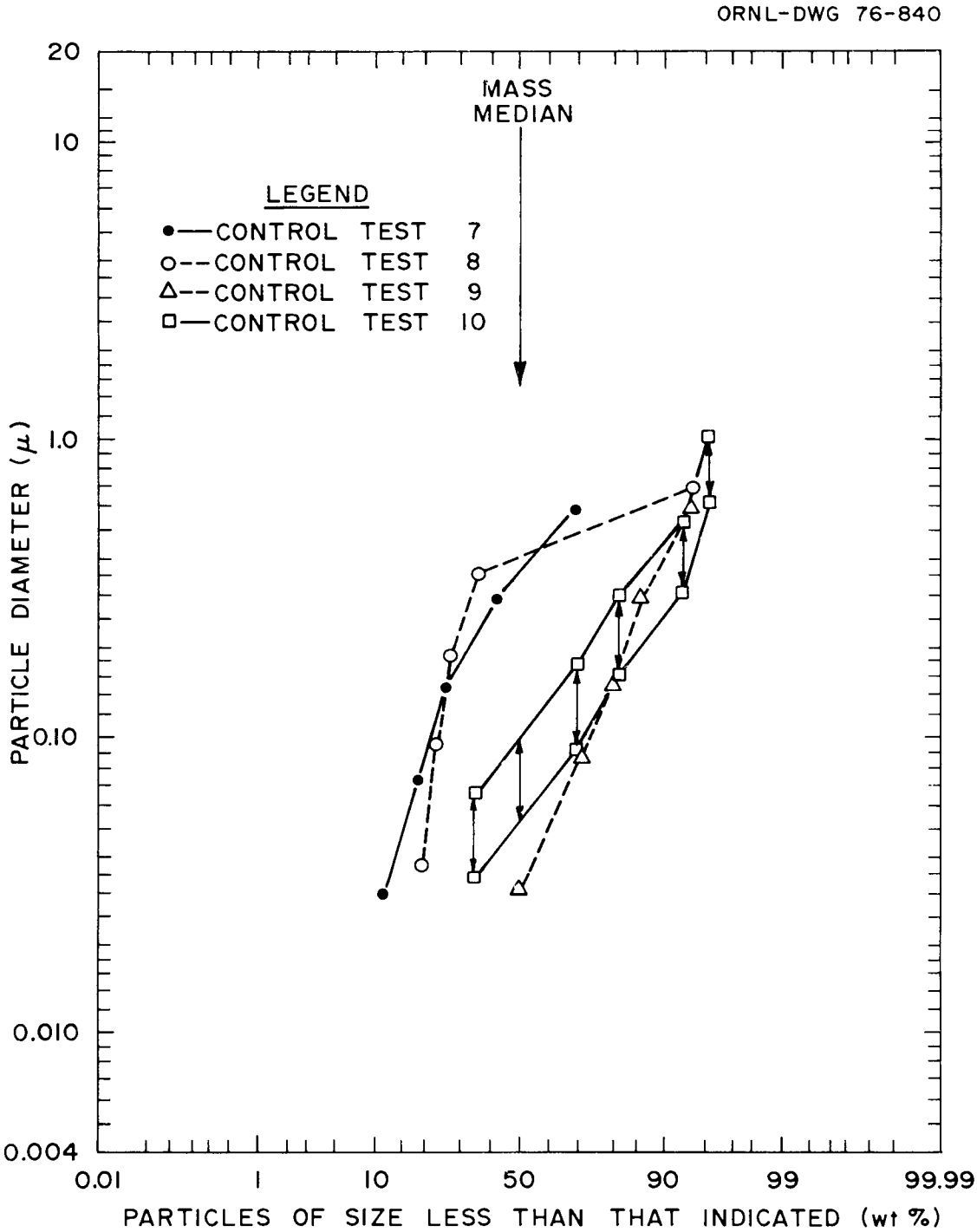

Fig. 8. Size distribution of cesium-containing particles.

4.3 Behavior of Cs_2O in Steam at 700, 800, and 950°C (Control Test 9)

Control Test 9 was performed in order to clarify the transport behavior of the Cs_2O reaction products as a function of temperature without interference by close contact with the fragments of the broken quartz ampules. In this test, the source material was loaded into a platinum boat, which was placed in the center of the furnace tube while in an argon atmosphere. The temperature of the furnace tube was quickly raised to 700°C and an 80% steam--20% argon atmosphere provided. No ^{137}Cs activity was detected in the collection system prior to introduction of the steam. The furnace tube was heated at 700, 800, and 950°C for 1-hr periods while the collection system was continually scanned with a recording gamma spectrometer. After the steam had been turned on, the ^{137}Cs activity in the thermal gradient tube increased more or less steadily as the temperature of the furnace tube was increased. The counting accuracy, however, was not good because of a low count rate. Significant activity above background was not measured until the furnace temperature reached 800°C; the cascade impactor activity increased steadily after this temperature level was attained. Deposits taken from the thermal gradient tube were identified by x-ray diffraction to be $CsOH \cdot xH_2O$. The double-peaked cesium deposition profile that was obtained in the thermal gradient tube from this control test is presented in Fig. 9.

Figure 10 is a photograph of the furnace tube, showing how the furnace tube liner was attacked. The platinum boat is illustrated at the left; at the extreme right is a region of clear quartz in the thermal gradient tube that was protected by the gold foil liner. Some of the etched quartz was scraped loose and examined by an SEM. The scraped material consisted of flakes approximately 50 μ thick, with 10 to 20% of one side covered with hemispherical projections approximately 7 μ in diameter. Only silicon was detected by energy dispersive x-ray fluorescence analysis. Cesium was present throughout the etched area of the furnace tube (Fig. 10 and Table 3), but apparently below the limit of detection by the electron microscope analyzer.

In Control Test 9, fiberglass filter papers were used as collection media in the cascade impactor in an effort to ensure good sticking

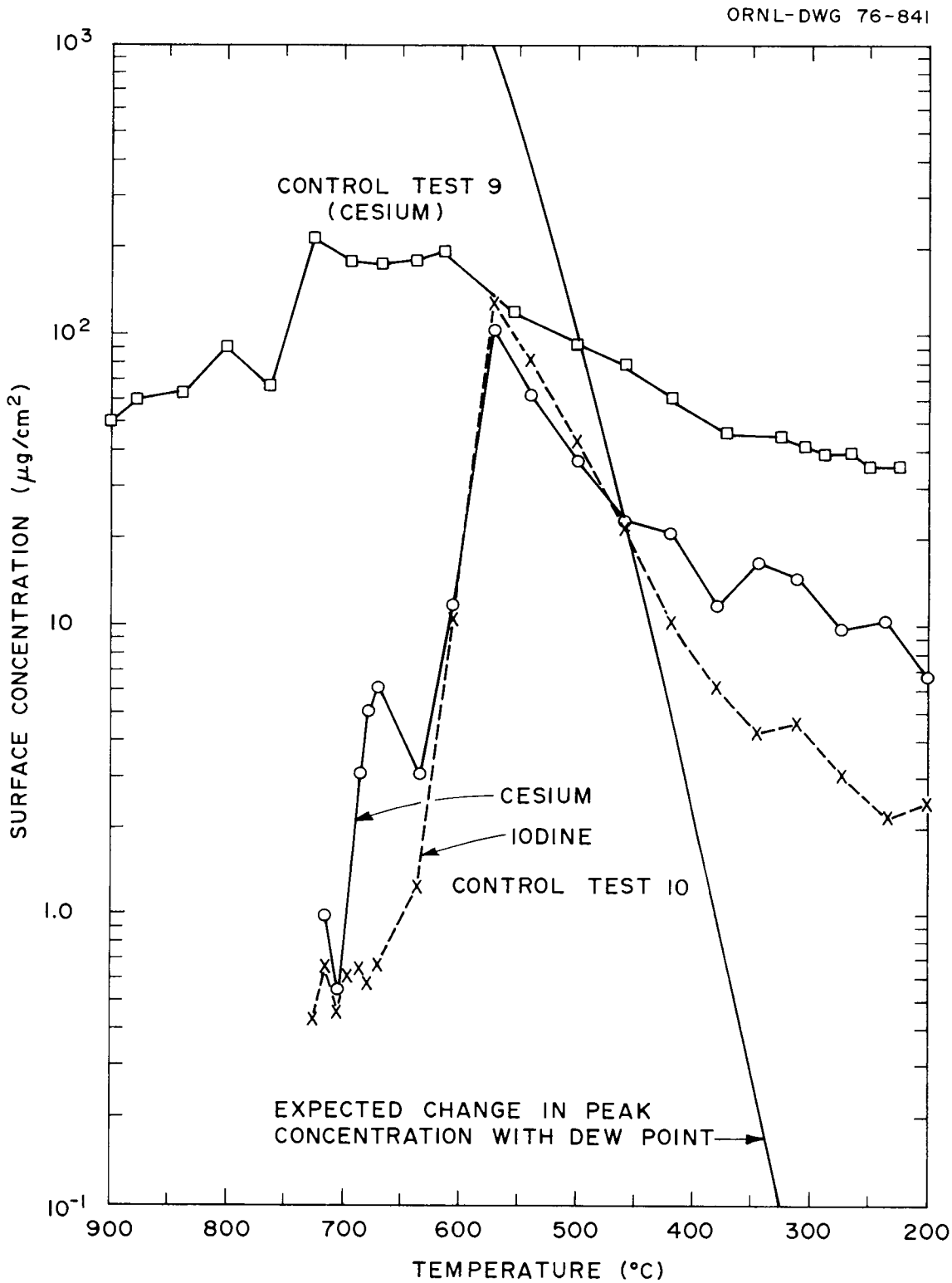

Fig. 9. Deposition of cesium-containing compounds in the thermal gradient tube.

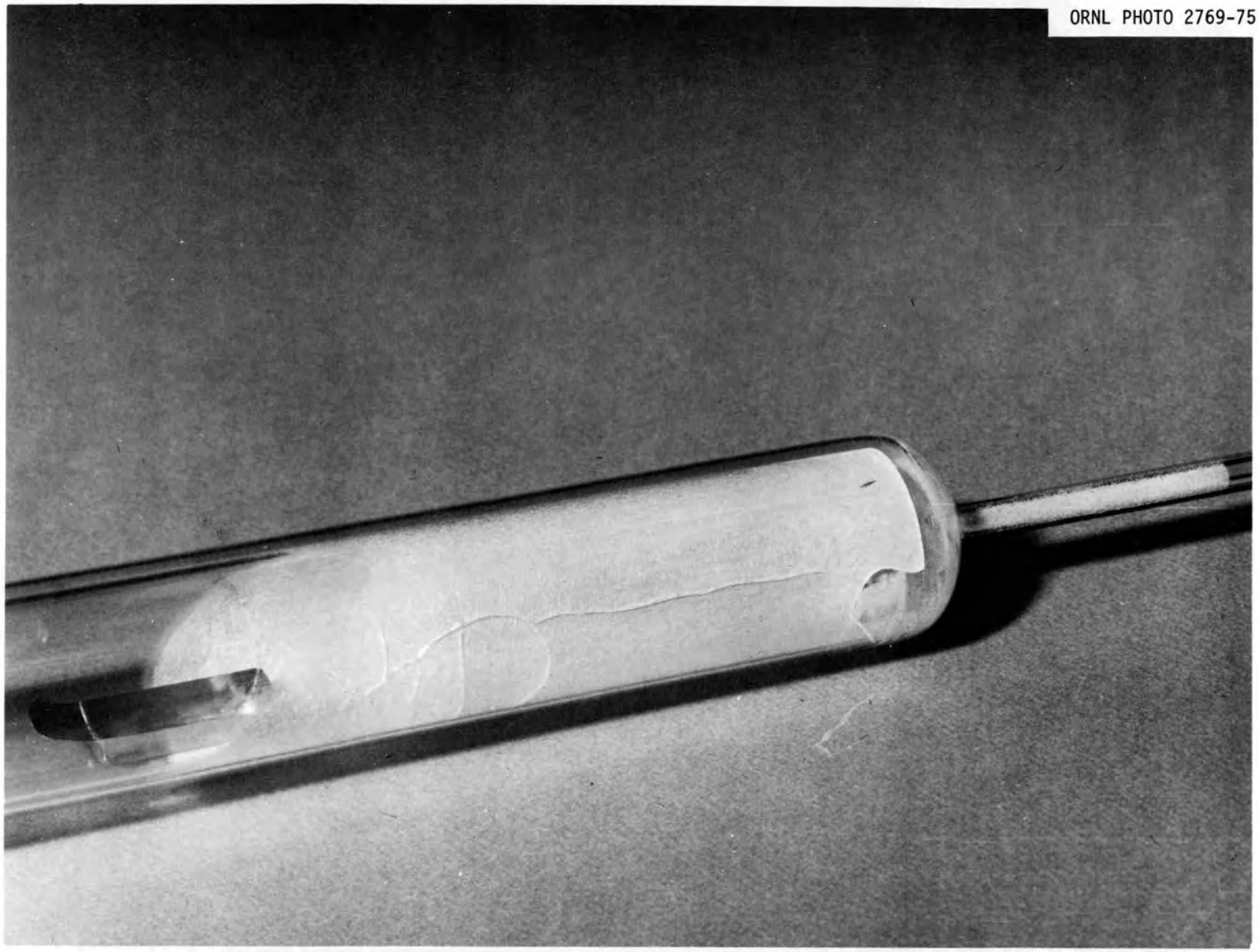

Fig. 10. Platinum boat, furnace tube, and entrance to thermal gradient tube at end of Control Test 9.

surfaces for the impacted particles in each stage. (We were not confident that the Teflon membrane papers were holding the particles efficiently.) Inspection of Table 3 and Fig. 6 shows that most of the particles were very small; the mass median diameter was approximately 0.03 μ, assuming a particle density of 3.6.

4.4 Conclusions

Cesium monoxide was found to react readily with steam to form cesium hydroxide which, in turn, reacted with the quartz furnace tube to form cesium silicates. The cesium that was transported to the collection system was generally deposited in the gold thermal gradient tube as cesium hydroxide. Most of the cesium that was transported beyond the thermal gradient tube was probably particulate matter, in the form of cesium silicate. As a result of our findings, we decided to use cesium hydroxide as one simulant of fission product cesium.

5. EXPERIMENT WITH CESIUM IODIDE

5.1 Introduction

Cesium iodide, which is considered to be thermally and chemically stable,[2-3] is a chemical form likely to be present in the fuel-cladding gap of a high-burnup fuel rod. Because of its volatility, this compound is a subject of interest in our studies. Table 4 is a summary of some of its properties.

5.2 Behavior of CsI in Steam at 700°C (Control Test 10)

Control Test 10 was conducted with a ^{134}Cs, ^{130}I-traced CsI sample which was placed in a quartz boat and positioned at the center of the furnace tube. The temperature of the sample was rapidly brought to 700°C under a reduced argon flow rate; then the argon flow rate was increased and steam injection initiated. The actual operating conditions are summarized in Table 1.

Table 4. Properties of CsI

Melting point	621°C
Boiling point	1280°C
Density	4.51 g/cc
Solubility	44 g/100 g H_2O at 0°C
ΔH_f at 25°C[a]	-80.5 kcal/mole
ΔH_{dissoc}[a]	100.0 kcal/mole
ΔH_{vap} (298)[a]	46.7 kcal/mole

Vapor pressures[b]

Temp. (°C)	324	376	433	496	565	656	750	894	1085
Pres. (torr)	10^{-6}	10^{-5}	10^{-4}	10^{-3}	10^{-2}	10^{-1}	10^{0}	10^{+1}	10^{+2}

[a] JANAF Thermochemical Tables.

[b] J. L. Margrave, The Characterization of High-Temperature Vapors, pp. 403-4, Wiley, New York, 1967.

Distribution data for both the cesium and the iodine nuclides are presented in Table 5. While most of the cesium remained in the furnace or was deposited in the thermal gradient tube, approximately one-third of the iodine (probably as elemental iodine) was carried into the impactor and deposited either on the aluminum surfaces of the impactor housing or on the silver screens. The cesium associated with the quartz boat was probably present as silicates. X-ray diffraction patterns that were obtained from material deposited on the fifth-stage collector in the impactor indicated approximately equal amounts of $CsOH \cdot xH_2O$ and CsI. On the basis of these observations, we conclude that approximately one-third of the CsI was decomposed to form I_2, cesium silicate, and cesium hydroxide. Figure 11 is a photograph (magnification 40,000X) of particulate matter on the fifth-stage filter paper of the cascade impactor using an SEM. An energy dispersive x-ray analyzer on the SEM revealed peaks of both cesium and iodine.

The radioactive iodine deposited in the furnace tube was located at the cooler inlet end (about 200°C). We believe that the iodine which deposited at this location was transported as CsI during the first few minutes by convective gas flow within the furnace tube before the steam flow started.

As is readily apparent from the data presented graphically in Fig. 9, both the cesium and the iodine nuclide concentration profiles in the thermal gradient tube show structure which strongly suggests deposition as CsI.

Iodine-130 activities in the thermal gradient tube and on the first silver screen are presented as functions of time in Fig. 12. Almost two-thirds of the iodine that was collected by the silver screen was deposited virtually instantaneously with steam injection, while the remainder accumulated at the rate of about 0.7% per minute (see Fig. 12). In contrast to the behavior observed on the silver screen, collection of the CsI in the thermal gradient tube proceeded much more slowly. About 75% of the CsI was deposited over a 15-min interval, and collection appears to have been complete at the termination of the test.

Table 5. Distribution of cesium and iodine in Control Test 10

	Temperature (°C)	Percent of total found		Mass (μg) Cs in most probable chemical forms			Mass (μg) I in most probable chemical forms		
		Cs	I	Cesium	CsI	$CsOH \cdot xH_2O$	CsI	I_2	Organic iodides
Quartz boat	700	23.38	1.61	145.93	10.77		10.29		
Furnace tube		40.36	33.66		225.25	45.16	215.09		
Thermal gradient tube	700-150	33.71	31.11		208.18	17.68	198.79		
Orifice assembly	175	0.57	1.85		0.94	2.88	0.95	10.87	
Impactor housing	175	0.78	10.10		1.21	4.02	1.15	63.39	
First-stage paper		0.05	0.09		0.07	0.27	0.07	0.51	
Second-stage paper		0.04	0.12		0.07	0.20	0.07	0.69	
Third-stage paper		0.13	0.47		0.20	0.67	0.19	2.81	
Fourth-stage paper		0.13	0.18		0.20	0.67	0.19	0.96	
Fifth-stage paper		0.40	0.26		0.67	2.01	0.64	1.02	
Filter pack housing	175	0.02	0.96			0.13		6.13	
First filter paper		0.41	0.13			2.75		0.83	
Second filter paper		0.003	0.17			0.02		1.09	
Third filter paper		0.001	0.04			0.01		0.25	
Silver screens, No. 1		0.003	18.05			0.02		115.33	
No. 2		0.001	0.39			0.01		2.49	
Nos. 3-12		0.002	0.44			0.01		2.81	
Adsorber housing	145	0.0	0.0						
Charcoals No. 1		0.0	0.37						2.36
No. 2		0.0	0.004						0.03
Other adsorbers		0.0	0.0						
Condenser housing		0.0	0.0						
Condensate	0	0.0	0.0						
Freeze trap	-78	0.0	0.0						
Cold charcoal trap	-78	0.0	0.0						
	Totals	100.0	100.0	145.93	447.56	76.51	427.43	209.18	2.39
				Total Cs = 670 μg			Total I = 639 μg		

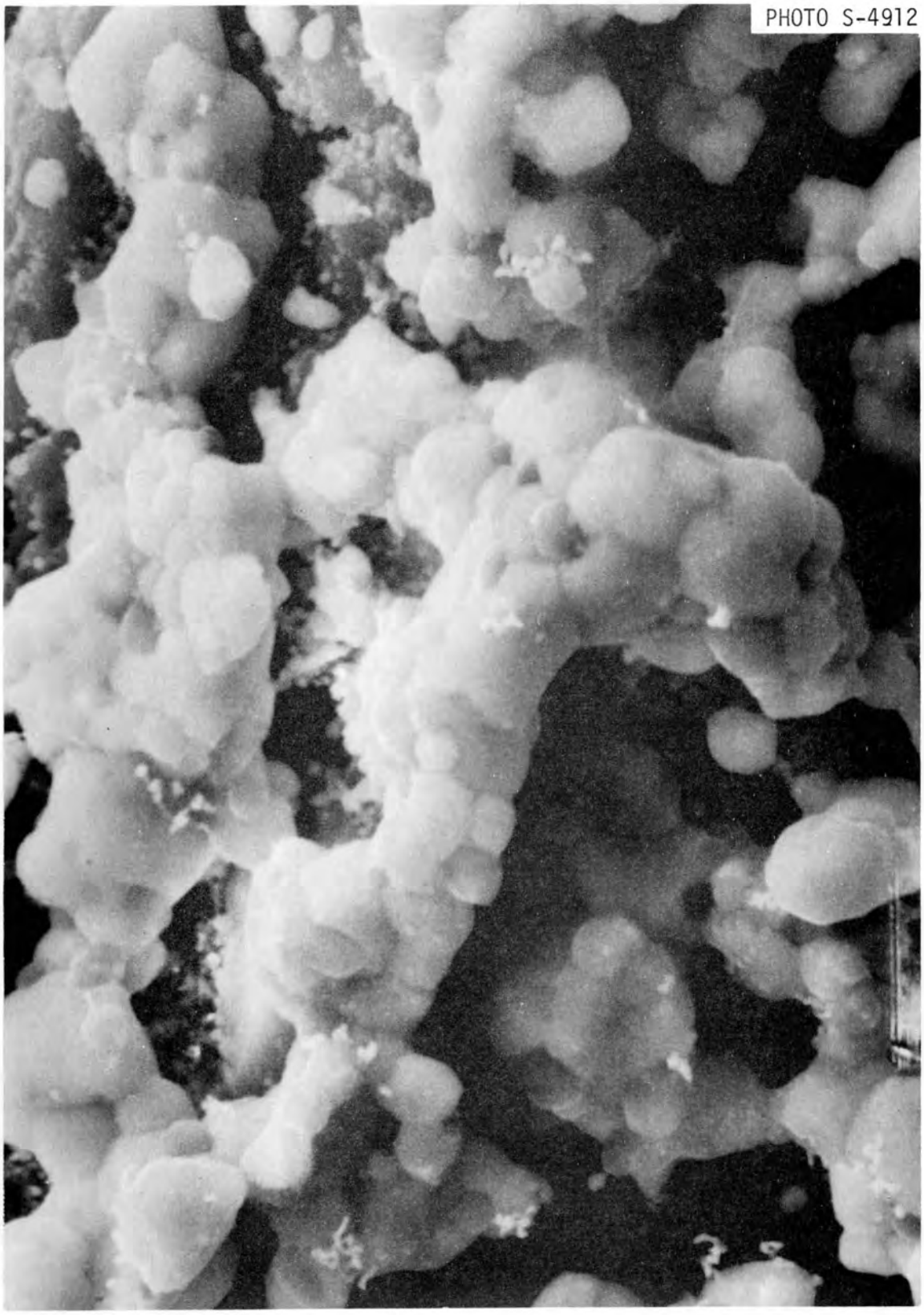

Fig. 11. Scanning electron microscope photograph of particles collected on impactor stage 5 of Control Test 10.

ORNL DWG 76-147

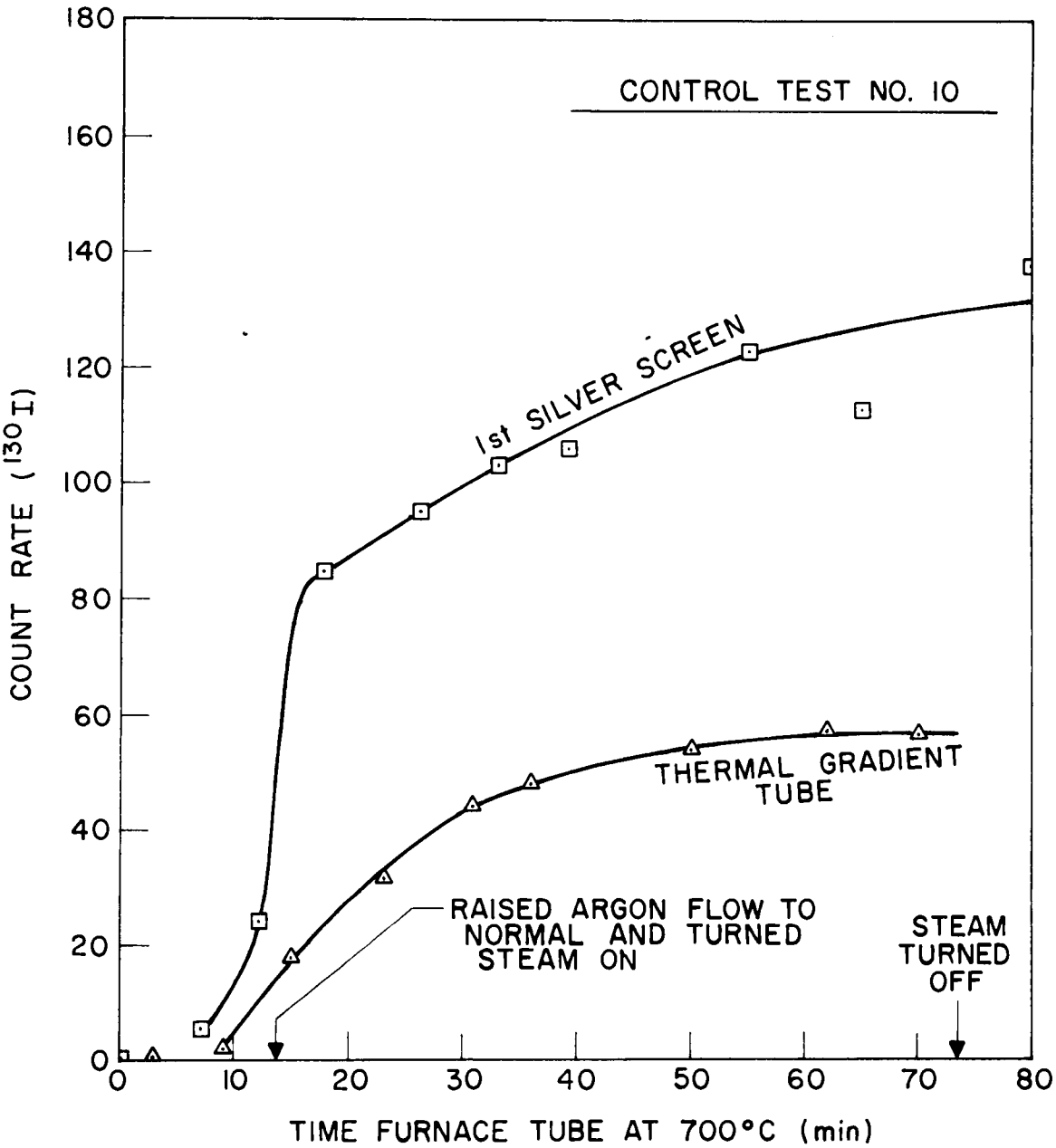

Fig. 12. Collection of radioactive iodine by the thermal gradient tube and silver screens of Control Test 10.

The particle size distribution is shown in Fig. 8 as a broad band since we were uncertain of the volume flow rate in this experiment. The indicated mass median size is in the range 0.05 to 0.1 μ, assuming a particle density of 3.6.

Although the significant decomposition of CsI which was noted in this test runs counter to the generally regarded[21] stability of CsI, we hasten to point out that the high release of iodine may be due to the reaction of the molten CsI with the quartz boat and the concomitant formation of cesium silicates.

6. PERFORMANCE OF THE APPARATUS

6.1 General Analysis

The apparatus performed quite satisfactorily. Most of the modifications, especially those made following Control Tests 1 and 2, were directed toward minimizing the plateout or adsorption of elemental iodine on extraneous surfaces. A broad distribution of iodine is only a minor nuisance as long as the element is radioactively traced; however, in future experiments using long-decayed, irradiated fuel capsules and rod segments, the only radioactive isotope of fission product iodine remaining will be ^{129}I, a very weak beta-emitter best detected by neutron activation to form ^{130}I (12.4-hr half-life). Where possible, we have used collection media that can be included in the activation analysis without interfering with induced activity. Examples are the Teflon membranes (used as impactor collection surfaces) and the special charcoal in the adsorber pack. Collectors such as the furnace tube, thermal gradient tube, metal components in the impactor, fiber glass filters, and silver-plated screens will have to be treated chemically to remove the ^{129}I for neutron activation analysis.

6.2 Quartz Furnace Tube and Quartz Liner

It is preferable for all of the material that is released from the control sample source (or fuel rod source in the case of fuel rod gap implant experiments and irradiated fuel rod experiments) to be transported quantitatively into the collection system, but it is obvious that the quartz furnace tube (liner) is quite reactive toward CsOH and

somewhat reactive toward CsI. Also, if the furnace tube is cooler than the condensation temperature for any compound, it will collect the material that condenses just as in the thermal gradient tube. This effect will become of greater importance when induction heating is used since only the metal fuel rod will be heated and the furnace tube temperature will lie between the rod and ambient temperatures.

One method of reducing deposition (and hence reaction) in the furnace tube would be to increase the flow rate, although this would affect the collection behavior of the other system components. We believe that our understanding of chemical behavior in the furnace tube is sufficient to compensate for these side effects. When monitoring the control sample source radioactively, deposition in the furnace tube has tended to mask release from the source (Control Test 9, for example).

6.3 Thermal Gradient Tube

We use the thermal gradient tube as a means of collecting compounds that will condense at temperatures above 125°C. Identification of the compound based on the deposition temperature is difficult because of its strong dependence on the instantaneous gas-phase concentration. Also, changes in the gas-phase concentration during the experiment may result in the start of a new deposition peak or partial evaporation of the original peak. Gas-phase mass transfer is not instantaneous and thus results in a peak that is broader than ideal, particularly at high gas velocities. Deposition by physical adsorption or chemisorption can occur with some compounds and with some thermal gradient tube materials. Castleman[24] and Collins[25] have used thermal gradient tubes to investigate fission products and simulants with moderate success.

The thermal gradient tube has performed quite satisfactorily as a collection device in our experiments. The thermocouples are located between the heater (Fig. 2) and quartz tube and therefore indicate only approximately the temperature of the gold foil liner. Table 6 shows the vapor pressure and corresponding gas phase concentration for saturated CsI vapor. The temperature at which the vapor begins to condense depends on its gas-phase concentration. For example, if the gas-phase concentration of CsI is 4.98×10^{-2} μg of CsI per cubic centimeter (565°C), CsI will begin to condense as soon as the gas is cooled below 565°C.

Table 6. Relationship of CsI dew point and mass of cesium or iodine transported

Dew point temperature (°C)	Vapor pressure (torr)	Saturated gas-phase concentration (μg CsI/cm^3 at temperature)	Mass of Cs or I transported in 1 hr at 350 cm^3 (STP)/min (μg)
565	10^{-2}	4.98×10^{-2}	1600
496	10^{-3}	5.42×10^{-3}	160
433	10^{-4}	5.91×10^{-4}	16
376	10^{-5}	6.43×10^{-5}	1.6
324	10^{-6}	6.98×10^{-6}	0.16

The mass of cesium or iodine transported in 1 hr at a typical experimental gas flow rate of 350 cm^3(STP)/min for this concentration would be 1600 μg. This material will condense in the thermal gradient tube with a peak concentration roughly equivalent to the total mass spread over perhaps 2 cm^2. This approximately allows us to generate a quasi-theoretical curve, shown in Fig. 9, for peak concentration vs dew point for CsI in a typical control test. (Notice that this anlysis depends on total gas flow.) A flow rate lower than that assumed (as with Control Test 10; see footnote in Table 1) would place the peak somewhat below or to the left of the theoretical curve.

6.4 Low-Pressure Cascade Impactor

Operation of an impactor at pressures below atmospheric permits the collection of smaller particle sizes as based on equations given by Parker and Buchholz.[26] At reduced pressures, the size of particles depositing on a given stage is more strongly dependent on particle density than when operating at atmospheric pressure. We assumed a particle density of 3.6 g/cm^3 (approximately that of CsOH) since much of the collected particulate material has been identified as $CsOH \cdot xH_2O$. Parker and Buchholz assumed a density of 4.0 for cesium-containing particulates, which is sufficiently close to 3.6 that size comparisons can be made directly with their data.[26,27]

We have used several different collection media in an effort to obtain reasonably good adhesion of impacted particles on a surface that would permit direct examination by x-ray fluorescence and neutron activation without excessive background or introduction of contaminants to the experimental system. Our first choice was Teflon membrane provided we could show satisfactory adherence of the particles. Several alternative materials were tried, including fiber glass filter media (in Control Test 9) without significant difference in deposit concentration being observed. The similarity in size distribution for Tests 9 and 10 (fiber glass and Teflon, respectively) demonstrated satisfactory performance of the Teflon membrane, even though the distribution of particle sizes is wider than usually observed. A log-normal size distribution would appear as a straight line in Fig. 8. The spread of sizes for log-normal distribution is indicated by the standard deviation, σ_g, which may be obtained as follows:[28]

$$\sigma_g = \frac{\text{84.13 percent size}}{\text{50 percent size}} \quad \text{or} \quad \sigma_g = \frac{\text{50 percent size}}{\text{15.87 percent size}} \quad .$$

Many log-normal aerosols have σ_g values in the vicinity of 2.0, but our value appears to be higher. The size distributions resulting from our experiments are apparently bimodal (i.e., a mixture of two different-sized aerosols) instead of simple log-normal. The large size centers around 1 μ in diameter and the small around 0.02 μ. We might continue the speculation and suggest that the larger particles are formed by a physical fracturing process, while the smaller ones are formed by vapor condensation.

6.5 High-Efficiency Filters

Keller et al.[29] demonstrated that, at 21°C with either low elemental iodine concentration or high relative humidity, particulate filter media could retain a large fraction of the I_2 by adsorption. Bennett et al.[4] found high retention of I_2 by adsorption at 90°C and 90% relative humidity. Examination of their original notebooks revealed that scatter in the latter data was probably a result of imprecise humidity control. Neither work investigated the reversibility of the I_2 adsorption.

We have found that the adsorption of I_2 on the filter media used in our experiments is usually less than 2% per layer (see Table 7). The low adsorption shown permits most of the I_2 to pass through to the silver-plated screens. The amount of iodine associated with particulates can generally be determined by subtracting the (adsorbed) iodine content of the second filter.

6.6 Silver-Plated Screens

In each of the experiments reported here, we used 80 mesh silver-plated copper screen that had just been cleaned with dilute KCN. Bennett[4] tested smaller-diameter 80 mesh silver-plated screens at 90°C and found good efficiency at loadings as high as 400 μg (corrected to our size). He found a lower efficiency when the loading was below 13 μg (corrected to our size) and suspected that this was due to the presence of unreactive forms of iodine such as CH_3I. We agree with his analysis.

At high iodine loadings, as seen in Fig. 4, our silver-plated screens showed reduced efficiencies that we interpret to be the result of saturation of the surface. At 400 μg the iodine deposit is equivalent to 58 monolayers (assuming 0.3 μg of I_2 per square centimeter per monolayer and a smooth plated surface with roughness factor of 1.0). The total iodine released in most projected fission product release experiments will be less than 400 μg.

Two alternative methods for nondestructive analysis of iodine on the screens were investigated for possible later application to the analysis of low-radioactivity iodine released from long-decayed samples of irradiated fuel. Direct counting of ^{129}I beta decay using a 4π beta counter indicated the presence of 9.3 μg of ^{129}I on the first screen of Control Test 10. Since the iodine used in our tests contained only 10% ^{129}I, the total iodine would be 93 μg, which compares well with the 115 μg shown in Table 5. This method cannot be used if interfering radioactivity is present and probably requires empirical adjustment for shielding of the low-energy beta rays by the screen itself.

Table 7. Adsorption of elemental iodine (I_2) on single high-efficiency filter papers[a]

Test number	Incident I_2 (μg)	Adsorbed I_2 (μg)	I on one paper (% of incident)
Control 1	450	162	36.1[b]
Control 2	620	41.	6.6
Control 3	1220	29	2.4
Control 4	2360	7.0	0.30
Control 5	274	0.99	0.36
Control 6	3850	5.3	0.14
Control 10	123	0.96	0.78
Implant 1[c]	4.1	0.024-0.48	0.59-11.7
Implant 2[c]	1.60	0.023	1.4
Implant 3[c]	0.81	0.0056	0.69

[a]Papers were 2.7 cm in diameter. Controls 1-4 used Cambridge 1G medium CM No. 115 fiber glass-asbestos. The remaining experiments used Reeve Angel 934 AH pure borosilicate glass fiber filters.

[b]These particular papers were 6.3 cm in diameter and contained 5.4 times the face area of other papers.

[c]R. A. Lorenz, J. L. Collins, and S. R. Manning, Quarterly Progress Report on Fission Product Release from LWR Fuel for the Period October-December 1975, ORNL/TM-5290 (March 1976).

The other method tested was x-ray fluorescence using the first screen of Control Test 6. The front surface was counted, and the reported iodine concentration was 50 $\mu g/cm^2$. Using the face area of 6.4 cm^2 gives a total iodine content of 320 μg. Our mass balance indicated that the total iodine content was 560 μg. A satisfactory quantitative measurement could probably be obtained by measuring both the front and back faces of the screen. This method is not considered to be as sensitive as the 4π beta counting.

6.7 Adsorbers

Control Test 5, in which CH_3I was passed through the 500°C furnace tube, showed the highest efficiency for trapping of radioactive CH_3I by the extra fine grain (12-16 mesh) 5% TEDA-impregnated charcoal. We selected this charcoal because of its low level of contaminants (375 ppm of sodium, 36 ppm of aluminum, 128 ppm of chlorine, 8700 ppm of potassium, 12.5 ppm of manganese, and 1.4 ppm of ^{127}I) that would interfere with direct neutron activation for determination of ^{129}I (and possibly ^{127}I) fission products. We should be able to detect 0.1 μg or more of ^{129}I, which is sufficient sensitivity for our experiments.

Unusually low trapping efficiency was experienced in several tests: Control Tests 3 and 6, and two Implant Tests performed after the control series. The cause of these poor results has been traced to overheating of the charcoal adsorbers (to the vicinity of 150°C) during the heatup phase of the experiments, which apparently allowed some of the TEDA impregnant to desorb, at least from the first cartridge.

The efficiency of adsorption during several control experiments is shown in Fig. 13. When operated properly, the first cartridge was capable of collecting essentially all of the CH_3I; the second cartridge completed the collection. The iodine penetrating the first two cartridges was probably an organic iodide form other than CH_3I. The silver-exchanged type 13X zeolite (AgX, at least 95% exchanged), 12-16 mesh, was included since we had observed in other experiments that AgX was more efficient than impregnated charcoal for trapping at least some forms of highly penetrating iodine. This capability to be confirmed by these control tests.

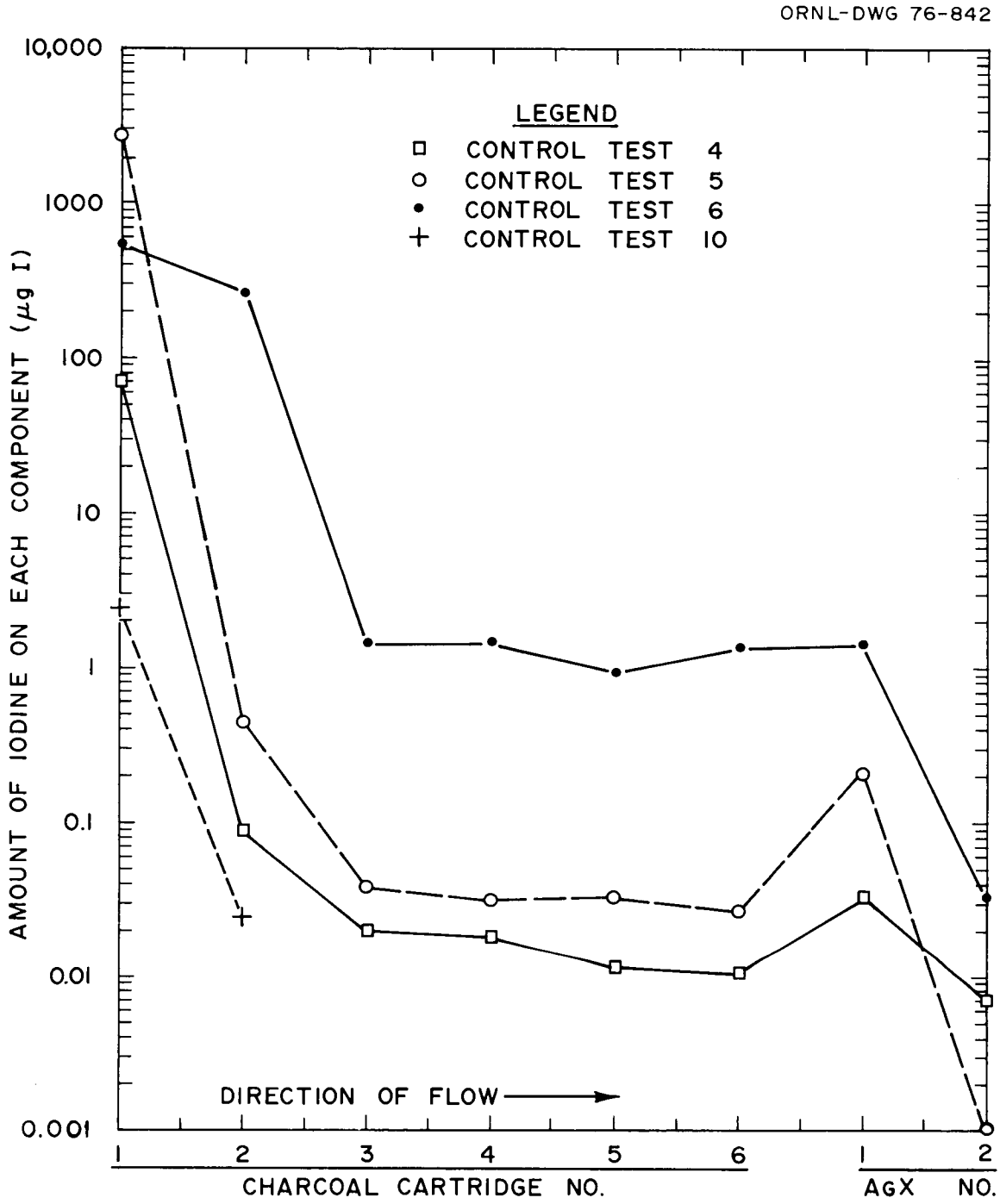

Fig. 13. Iodine distribution in the adsorber packs.

We have compared our adsorption efficiency with that measured by May and Polson[30] in Fig. 14. The "tenth thickness" is the depth of adsorber that reduces the radioactivity by a factor of 10. The efficiency of an adsorber is dependent on a long list of parameters, including velocity, relative humidity, degree of moisture equilibrium, pressure, temperature, purging, possible overload, impregnant, base charcoal, grain size, void fraction, age before use, and service history. The relatively simple evaluation afforded by Fig. 14 should enable us to differentiate between compounds similar to CH_3I and others that are more difficult to collect.

7. APPLICATION OF RESULTS

7.1 Application to Future Experiments with H. B. Robinson Irradiated Fuel

We have calculated that the amount of fission gas released to the plenum and pellet-clad gap of the H. B. Robinson fuel was only approximately 0.24% of the total in the rod.[22] If the same fraction of iodine were released from the pellets to the gap region, the iodine content of the gap should be approximately 100 μg per 12-in. length (the length that we plan to use in future fission product release experiments). Since we anticipate a gap escape fraction of the order of 1% for some of the lower temperature release experiments, the released iodine will amount to only 1 μg, more or less.

In order to measure this amount of iodine (mostly ^{129}I) reliably, we plan to eliminate nonessential components from the collection system and minimize the remaining components, where possible, to reduce the extraneous adsorption of iodine. Since particulate material does not normally appear in low-temperature experiments, we could logically eliminate the impactor and, in turn, the orifice plate. Two high-efficiency filters should be retained, however. Elimination of the silver-plated screens would sacrifice determination of the elemental iodine/organic iodide ratio, but all of the iodine could be collected by the charcoal and thus be available for direct, nondestructive neutron activation analysis.

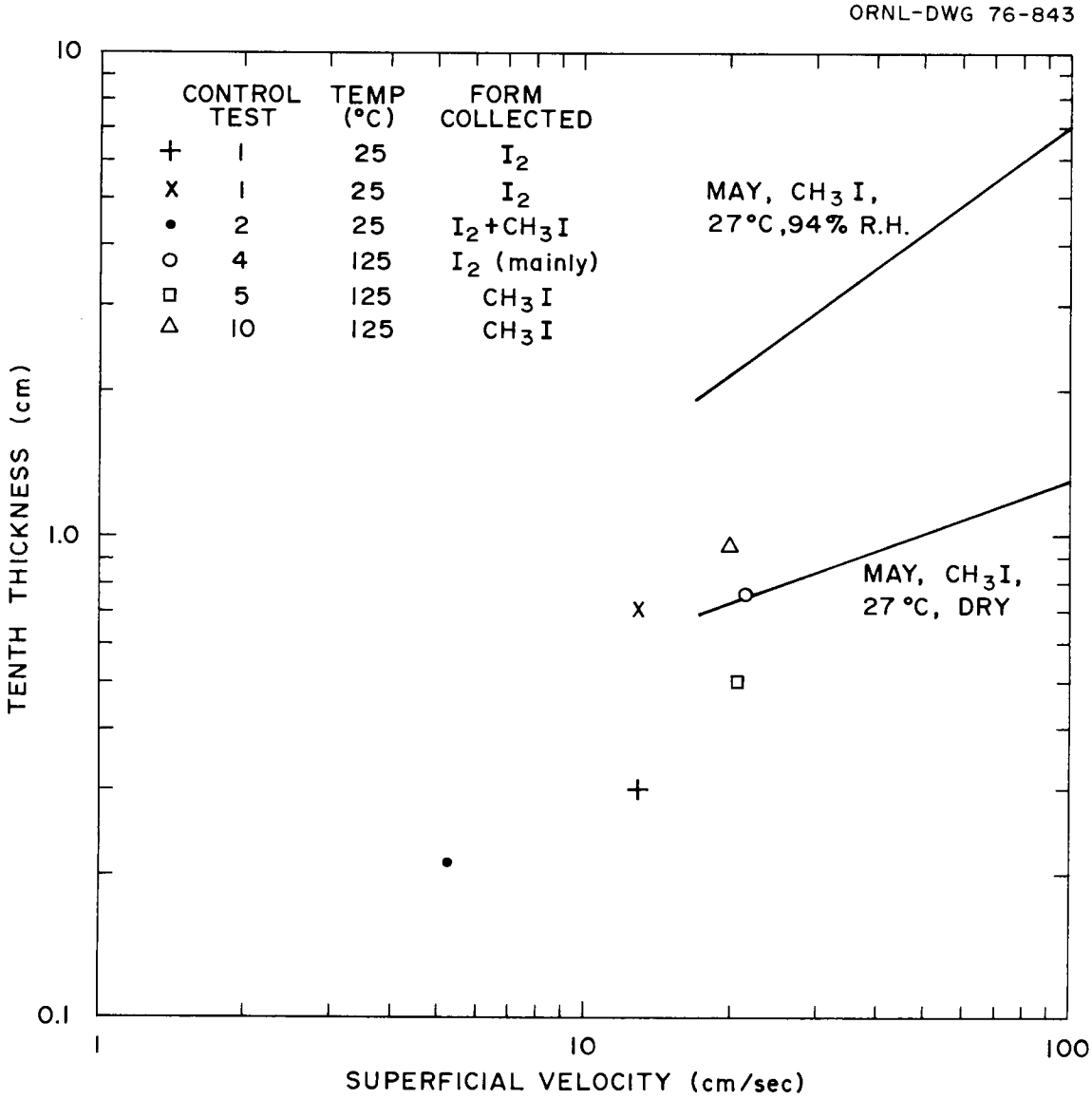

Fig. 14. Efficiency of charcoal for trapping radioactive iodine.

7.2 Application of Results to Reactor Safety Analysis

The series of tests described here was performed primarily to determine the optimum equipment arrangement and to provide background information for analysis of future experiments using fuel rod segments; however, at least two general observations are pertinent.

Although thermal decomposition (pyrolysis) of CH_3I is nothing new in itself, we believe that our rate data are the first published for steam atmospheres. Apparently the thermal decomposition rate is not significantly affected by steam. High-temperature situations in which the thermal decomposition of methyl iodide might be controlling are LOCAs (within the primary vessel) and spent fuel accidents if the fuel rods or cask should heat up to the order of 400°C. The total rate of destruction of CH_3I should be a combination of thermal effects, beta-gamma radiation, and photolysis (sunlight). In any situation, the rate of destruction must be balanced against the principal rate of formation of CH_3I, which is usually gas-phase beta-gamma radiation (strongly dependent on the concentration of methane and other organic material). Postma and Zavadoski include a good review of available data.[9]

Another point of practical importance is the well-known rapid reaction of cesium and cesium oxides with moisture to form cesium hydroxide. Because of computer capacity limitations, this reaction was apparently omitted from a recent thermodynamic study of fission product chemical forms expected within fuel rods and after release to a steam environment.[31] Although this reaction would not affect the conclusions of the study, we believe that it should be included in future thermodynamic studies of cesium behavior.

8. REFERENCES

1. R. C. Brasted, Comprehensive Inorganic Chemistry, Vol. III, "The Halogens," Van Nostrand, New York, 1954.

2. G. W. Keilholtz and C. J. Barton, Behavior of Iodine in Reactor Containment Systems, ORNL-NSIC-4 (1965), p. 3.

3. M. F. Osborne, E. L. Compere, and H. J. de Nordwall, Studies of Iodine Adsorption and Desorption on HTGR Coolant Circuit Materials, ORNL/TM-5094 (1976), p. 48.

4. R. L. Bennett and R. E. Adams, "Development of a Sampling Device for Distinguishing the Forms of Iodine in a Humid Atmosphere," pp. 235-61 in Proceedings of the 10th AEC Air Cleaning Conference, New York, August 28, 1968, USAEC Report CONF-680821.

5. H. S. Rosenberg, J. M. Genco, and D. L. Morrison, Fission Product Deposition and Its Enhancement Under Reactor Accident Conditions: Deposition on Containment-System Surfaces, BMI-1865 (May 1969).

6. G. W. Keilholtz and C. J. Barton, Behavior of Iodine in Reactor Containment Systems, ORNL-NSIC-4 (1965), p. 54.

7. R. E. Adams, R. D. Ackley, and R. P. Shields, "Application of Impregnated Charcoals for Removing Radioiodine from Flowing Air at High Relative Humidity," p. 398 in Treatment of Airborne Radioactive Wastes, Proceedings of a Symposium, New York, 26-30 August 1968, IAEA, Vienna, 1968.

8. A. G. Evans, Confinement of Airborne Radioactivity, Progress Report: July-December 1972, USAEC Report DP-1329 (June 1973), pp. 10-16.

9. A. K. Postma and R. W. Zavadoski, Review of Organic Iodide Formation Under Accident Conditions in Water-Cooled Reactors, WASH-1232 (1972).

10. L. H. Gevantman and R. R. Williams, "Detection and Identification of Free Radicals in Radiolysis of Alkanes and Alkyl Iodides," J. Phys. Chem. 56, 569-74 (1952).

11. H. W. Thompson and J. W. Linnett, "The Vapour Pressures and Association of Some Metallic and Non-Metallic Alkyls," Trans. Faraday Soc. 32, 681-85 (1936).

12. L. C. Schwendiman, J. Mishima, A. K. Postma, L. L. Burger, and R. A. Hasty, The Washout of Methyl Iodide by Hydrazine Sprays Progress Report (Through September 1967), BNWL-530, pp. 18-19.

13. L. F. Parsly, Chemical and Physical Properties of Methyl Iodide and Its Occurrences Under Reactor Accident Conditions, ORNL-NSIC-82 (1971), pp. 3-11.

14. E. T. Butler and M. Polanyi, "Rates of Pyrolysis and Bond Energies of Substituted Organic Iodides," Part I, Trans. Faraday Soc. 39, 19-36 (1943).

15. C. Horrex and R. Lapage, Disc. Faraday Soc. 10, 233-34 (1951).

16. E. W. R. Steachie and R. D. McDonald, "The Kinetics of the Thermal Decomposition of Gaseous Methyl Iodide," J. Am. Chem. Soc. 57, 488 (1934).

17. E. A. Moelwyn-Hughes, "The Hydrolysis of the Methyl Halides," Proc. Roy. Soc. (London) A-164, 293-306 (1938).

18. H. L. Finston and M. T. Kinsley, The Radiochemistry of Cesium (Nuclear Science Series), NAS-NS 3035 (1961), pp. 11-13.

19. J. C. Bailar, Jr., Comprehensive Inorganic Chemistry, Vol. 1, pp. 423-27, Pergamon, New York, 1973.

20. George Brauer, Handbook of Preparative Inorganic Chemistry, Vol. 2, 2nd ed., pp. 1220-21, Academic, London-New York, 1965.

21. J. C. Bailar, Jr., Comprehensive Inorganic Chemistry, Vol. 1, pp. 467-69, Pergamon, New York, 1973.

22. R. A. Lorenz et al., Quarterly Progress Report on Fission Product Release from LWR Fuel for the Period October-December 1975, ORNL/TM-5290 (March 1976), pp. 34-35.

23. B. D. Epstein, A Review of the Literature Pertinent to Fission Product Migration and Interaction in Fuel Rods, GA-A13423 (1975), p. 13.

24. A. W. Castleman, Jr., I. N. Tang, and H. R. Munkelwitz, Chemical Reactions and Transport Behavior of Fission-Product Iodine, CONF-650407 (April 1965), pp. 325-43.

25. D. A. Collins, R. Taylor, and W. D. Yuille, Sampling and Characterization Techniques Used in the Study of Iodine Release from Irradiated Fuel Elements, CONF-650407 (April 1965), pp. 1096-1117.

26. G. W. Parker and H. Buchholz, Size Classification of Submicron Particles by a Low-Pressure Cascade Impactor, ORNL-4226 (June 1968).

27. G. W. Parker, G. E. Creek, and W. J. Martin, Fission Product Transport and Behavior in the Stainless Steel Lined Containment Research Installation (CRI), ORNL-4502 (February 1971).

28. H. L. Green and W. R. Lane, Particulate Clouds: Dusts, Smokes, and Mists, Van Nostrand, Princeton, N.J., 1964.

29. J. H. Keller, F. A. Duce, and F. O. Cartan, Retention of Iodine on Selected Particulate Filters and a Porous Silver Membrane Being Considered for the LOFT MAYPACK, IN-1078 (May 1967).

30. F. G. May and H. J. Polson, Methyl Iodide Penetration of Charcoal Beds: Variation with Relative Humidity and Face Velocity, AAEC/E-322 (September 1974).

31. Reactor Safety Study, An Assessment of Accident Risks in U. S. Commercial Nuclear Power Plants, WASH-1400 DRAFT, Appendix E of Appendix VII.

ORNL/NUREG/TM-25
NRC-3

Internal Distribution

1. M. Bender
2. C. J. Borkowski
3. J. O. Blomeke
4. K. B. Brown
5. J. R. Buchanan
6. J. B. Cathcart
7. C. F. Coleman
8. W. B. Cottrell
9-14. J. L. Collins
15. F. L. Culler
16. G. G. Fee
17. D. E. Ferguson
18. M. H. Fontana
19. H. W. Hoffman
20. G. Hofmann
21-24. R. A. Lorenz
25. F. C. Maienschein
26-35. A. P. Malinauskas
36. D. L. McElroy
37. C. J. McHargue
38. F. H. Neill
39-40. M. F. Osborne
41. G. W. Parker
42. H. Postma
43. L. B. Shappert
44. D. B. Trauger
45. B. L. Vondra
46. J. R. Weir
47. R. G. Wymer
48-49. Central Research Library
50. Document Reference Section
51. Laboratory Records - RC
52-56. Laboratory Records Department
57. ORNL Patent Section
58. W. K. Davis (Consultant)
59. J. C. Frye (Consultant)
60. C. H. Ice (Consultant)
61. R.B. Richards (Consultant)
62. D. O'Boyle (Consultant)

External Distribution

63-71. Director, Division of REactor Safety Research, Nuclear Regulatory Commission, Washington, D. C. 20555
72. Director, REactor Division, ERDA, ORO
73. Director, Research and Technical Support Division, ERDA, ORO
74. J. Sisler, ERDA/ECT
75. K. Campe, NRC/NRR
76. W. Lahs, NRC/RES
77. D. Hopkins, NRC/OSD
78-397. Given distribution as shown in category NRC-3

☆ U.S. GOVERNMENT PRINTING OFFICE: 1976-641-252/425